THEORETICAL AND COMPUTATIONAL MODELING OF THE EFFECTS OF ELECTROMAGNETIC FIELD ON THE PLASMODIUM FALCIPARUM

A Thesis Submitted to

AFRICAN UNIVERSITY OF SCIENCE AND TECHNOLOGY

(AUST-ABUJA)

In partial fulfilment for the award of

MASTERS DEGREE IN THEORETICAL PHYSICS

BY:

JULIET SACKEY

Supervised By:

PROF. WOLE SOBOYEJO

Princeton Institute of Science and Technology of Materials (PRISM)

Princeton University

December, 2011

Dedication

I dedicate this work to Almighty God who saw me through my studies here and also to my family and siblings.

Declaration

I thereby declare that the matter embodied in this thesis "THEORETICAL AND COMPUTATIONAL MODELING OF THE EFFECTS OF ELECTROMAGNETIC FIELD ON THE PLASMODIUM FALCIPARUM'' is the result of the investigation carried out by me under the supervision of Prof. Wole Soboyejo at the African University of Science and Technology and that it has not been submitted elsewhere for the award of a degree or diploma.

In keeping with the general practise in reporting scientific observation, due acknowledgement has been made whenever describe is based on findings of other investigators.

……

JULIET SACKEY

Acknowledgements

First and foremost, I thank God for inspiring and motivation me in difficult time while undertaking this work. It is by His grace and mercy; I was able to complete this work. Most of all, I wish to thank the AUST Care Group fellowship where I derive my encouragement and spiritual support from during challenging moment here. Also I appreciate my parents who encourage me during my stay here. Aryeetey, Emmanuel has also be so wonderful to me, providing me with all the confront I needed to complete my studies here, I say thank you very much. My profound gratitude goes to my supervisor Prof. Wole Soboyejo who advice and supervised me for this work to be completed successfully. I also expressed my gratitude to the staff and students at African University of Science and Technology. My appreciation also goes to my colleagues in the theoretical Physics Stream especially Jonas Bugase, my friends and to you, Justice Archer

Abstract

The study explores the potential effects of the remote application of cyclic magnetic field to the female anopheles mosquitoes that carry malaria parasites. The goal is to develop a theoretical basis that can guide the cyclic activation of the magnetic field to induce the inactivity of the malaria parasite without killing the mosquitoes. The model considers the hemozoin within the malaria parasite as a cluster of magnetic nanoparticels. The potential effects of the applied magnetic field are then considered within a thermodynamic frame framework. The induced heat generated is computed implicitly within a combined analytical and computation approach. From our numerical analysis, we noticed that, an increase in the frequency with a strong magnetic field causes heating of the magnetic nanoparticles. Experimentally, in a magnetic field induction of 0.3 T, the protein in the heme acquire enough energy to survive at a temperature of 24^{o}C with a frequency of 4.2 kHz and the volumetric power dissipated of $956.6890 W/m^3$ in 300 s window. A numerical simulation based on finite element scheme was employed to reaffirm this analysis. At a maximum temperature of 42^{o}C, for 900s steady state, the bonds in the particle begin to break off destroying their tertiary structure as a result of the thermal agitation in a form of collision thereby losing it ability to stay inside the chamber. This therefore enables the release of the nanoparticle out of the chamber of the hemozoin into the plasmodium falciparum making it inactive of malaria transmission. The effects of the localised changes in temperature are discussed for potential applications in future devices that could be developed to render malaria parasites inactive of transmission of malaria.

Contents

Chapter Three

Chapter Four

List of Symbols

H_o Magnitude of Magnetic field …….26

α Thermal diffusivity ……..18

u Temperature gradient ……..18

Ω, Resonance frequency …….18

ω Driving frequency ……...19

ω_0 Damping Constant……..19

Q Added Heat…….24

μ Magnetic Moment……12

ξ_1 Constant…….19

List of Figures

Chapter one

Background and Introduction

1.1 Background and Introduction

The World Health Organization (WHO) estimates that 250 million people were infected annual with malaria. This result in approximately 10 million death annual [1] with over 300.000 Nigerian being infected each year[2]. In 2000, 91% of death in Africa is as a result of malaria infection, out of which 85% are children under the age of 5 years [3]. This results in 35 countries responsible for the majority of death in world -wide. Nigeria, Democratic Republic of Congo, Uganda, Ethiopia, and Tanzania are five main contributors of death as result of malaria infection. WHO estimated that 50% of global death and 47% cases are from those countries [4]. The average number of work days lost per malaria episode in a household was found to be 16 days in agrarian household and 15 days in non-agricultural segment[2] The figure below illustrate the average number of days of work loss of the adult in Africa[5]. In most cases, the effort to treat malaria have relied on the use of drugs such as combination therapies of artemisinin and established malaria drugs such as those of the quinoline family [45]. However, these drugs are relatively expensive [48] and well beyond the reach of the people living on less than $1-2/day. Furthermore, although the use of insecticide treated nets has been shown to be effective in reducing the incidence of malaria [4], there are still major concerns about the potential for malaria infection in areas with relatively high levels of female anopheles mosquitoes. The four different types of Plasmodium parasite are

- Plasmodium falciparum- this is the only parasite that causes malignant malaria. It causes the most severe symptoms and results in the most fatalities.
- Plasmodium vivax - this causes benign malaria with less severe symptoms than *P.*

falciparum. P. vivax can stay in your liver for years and can lead to a relapse.

- Plasmodium ovale - this causes benign malaria and can stay in your blood and liver for many years without causing symptoms.
- Plasmodium malaria - this causes benign malaria and is relatively rare.

Each parasite causes a slightly different type of illness [6]. Malaria is caused by the infection of the red blood cells with protozoa. When an infected mosquito bites a person, it sucks up that person's blood and infects him or her with the disease. The infected person can then transmit the disease to the next female anopheles that takes the blood bite. This is what causes malaria's hallmark symptoms such as fever, uncontrolled shivering, aches in the joints and headache [7**]**. If blood is infected with parasites, it may be difficult for blood to flow crucial organs such as the brain. Pregnant women are also at risk since their chances of miscarriage and premature death of their babies are increased after infection with malaria [6].

Furthermore, in cases where the malaria is severe, there are a number of complications associated with. These complications could be kidney failure, low blood pressure, or possibly haemorrhage [8]. Today, malaria is one of the most invested endemic of all times [9]. According to the World Health Organization, "malaria may accounts for as much as 40% of public health expenditure, 30% to 50% of impatient admission and up to 50% of outpatient visits'' [10]. Resistance has been developed to single drug therapies, especially in countries in which the disease is endemic. There is therefore, the need for alternative approaches to the management of malaria in areas in which the malaria is endemic.

1.2 An Alternative Approach

Recent experimental work by Lai has showed that, the heating of the anopheles mosquitoes can be achieved by the cyclic application of magnetic field. However, the physics of the underlying

heating process is yet to be established. In spite of the application of the experimental result, there is the need to develop a theoretical physics base for the control of the future devices. These devices could be used to prevent infection with malaria parasites that are rendered harmless through the application of cyclic electromagnetic field.

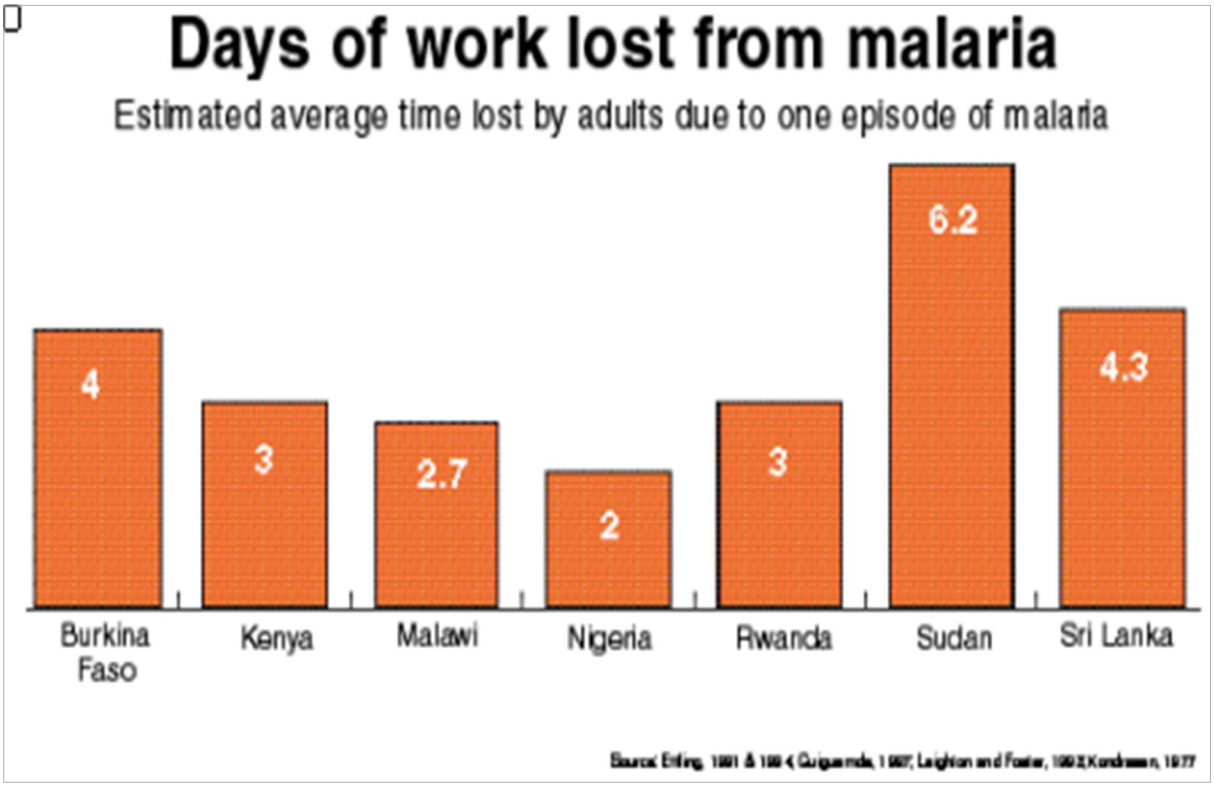

Figure 1.1: Days of work lost from malaria

1.3 Objectives and Scope of Thesis

The objective of this work is to use physics-based approach to model the effects of cyclic activated magnetic fields on the localized heating of the malaria infected tissue in the female anopheles mosquitoes. The project will be carried out in the following stages:

First, the hemozoin in the parasites will be idealized as clusters of magnetic nanoparticle that are embedded in the tissue. The potential effects of the cyclically activated magnetic field will then be modelled analytically within a thermodynamic framework.

The heat generation and diffusion due to the cyclically activated field then be modelled within a computational framework that will be implemented using finite element techniques.

The models will be validated using experimental results obtained by Solomon Abiola in previous work. The potential for the denaturation of the malaria parasites will also be elucidated in collaboration with an infectious disease group.

Chapter Two

2.0 Literature Review

2.1 Life Stages of the plasmodium parasite

The malaria parasites spend their life either in the erythemal primary host (human) or poikilothermal secondary host (anopheles mosquito) [73]. The plasmodium ingest 25 -75% of the host cell during the intraerythrocytic stage [50]. The female anopheles mosquito transfers the malaria parasite into the host in the process of feeding. The sporozoites travel through the blood stream and invade the liver cell where it develops within 5 – 10 days. During those stages, the sporozoites undergo asexually reproduction to form a tissue called schizont which later develops into merozoites. These merozoites rupture the liver cell and invade the red blood cell. Inside the RBC, the merozoites matured into trophozoites which further develop into schizont. These schizonts develop, divide and rupture from the RBC relasesing additional merozoites leading to begin another cyclic.

2.1.2 Haemoglobin Degradation

The malaria parasite has limited capacity to synthesis amino acid and therefore, it scavenges the host's nutrient [51]. Within the RBC, the plasmodium falciparum attain nutrients by degrading the heamglobin from the host. These heamglobin are then transported via a vesicle called cytosome into the acidic digestive food vacuole [47]. As a consequences, of the Hb degradation, a heme is released which also induces oxygen radicals. About 95% of the heme released is converted into hemeozoin [52].

2.1.3 Heme Polymerization

The heme detoxification is achieved by polymerizing the free heme into an insoluble crystalline material called hemozoin. Several heme – binding antimalarial compounds efficiently inhibit this process and this is the mechanism by which the drugs induce parasite toxicity [58]. Heme polymerase is located in the acidic food vacuole of pH 4.8- 5.3 [53] of the parasite and uses ferriprotoporphyrin IX (FP) as substrate for biosynthesis of hemozoin [54]. It is favourably in a high temperature of 70^0c [57]. Iron protoporphyrin IX is a ubiquitous molecule that is essential for the function of all aerobic cells [55]. The hemozoin has a structure similar to that of β-hematin in which ferric iron of one heme is coordinated to the propionate carboxylate group of the next heme. It can be identified by Fourier transform infrared spectroscopy with intense absorbance at 1664 cm^{-1}corresponding to C = O, stretching vibration and at 1210 cm^{-1}, corresponding to the C – O stretching vibration [56].

(a) Heme

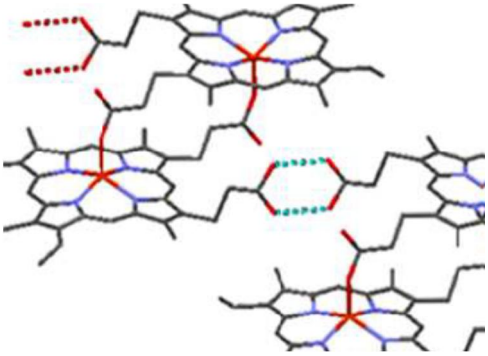

(b) Hemozoin

Figure 2.1: Chemical structure of:

2.1.4 Malaria Parasite

This research focus specifically on the hemozion in the malaria parasites. Research has shown that malaria parasites are vulnerable to free heme molecules which generate oxygen radicals. These free toxic hemes are released after haemoglobin catabolism in acidic lysosome-like organelles [4]. Several blood-feeding organisms have enveloped efficient adaptation to circumvent the toxic effect of the 'free heme'[45]. This process involves the crystallization of the heme into hemozoin [46]. These hemozion appears to be inactive with reference to biological consequence inside the parasite nevertheless the heme crystal has diverse modulatory effects on the immune system.

2.1.5 Hemozion

The Malaria parasite generates a super magnetic particle, known as hemozoin, during the process of feeding **[**11**]**. Hemozoin is the disposal product formed from the digestion of blood feeding parasite. It is formed within the acidic aqueous (pH 4.8) environment of the digestive food vacuole of the plasmodium falciparum [47]. Since the formation of the hemozoin is essential for the survival of these parasites, it is therefore an attractive target for developing drugs and is much studied in plasmodium as a way to find drugs to treat malaria. The hemzoin crystal is about 100-200 nm long and each contains about 80,000 heme molecule [49].

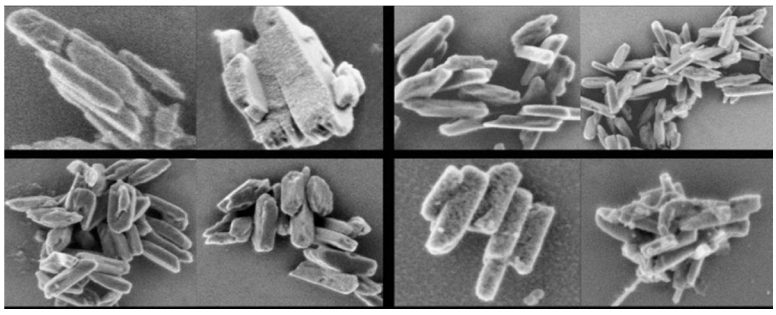

Figure 2.2 : SEM images of hemozoin nanocrystal

2.2 Oscillations of the Hemozoin

Oscillation is the repetitive variation between two or more different states. Oscillation occurs both in physics system and biological system [12]. When a mass is attached to a linear spring, subjected to no external force, such a system is said to be in equilibrium when the spring is static. However, when the system is displayed, there is a net restoring force which tends to bring it back to equilibrium, in this process, the mass acquire a momentum [13]. Current research in this field indicates that oscillating magnetic field could cause oscillation of the hemozoin, leading to a mechanical damage of the organelles of the parasite. Mechanical stresses are known to cause cell death via apoptosis [5].

2.3 Hysteresis

Hysteresis systems are path dependence, the output depends in part on the internal state of the system and not only on its input **[**14**].** If an alternating a magnetic field is applied to a material, its magnetization will trace out a loop called hysteresis loop [14**].** Therefore a hysteresis loop shows the relationship between the induced magnetic flux density and the magnetizing force [15]. By studying the hysteresis loop, much information on the magnetic property of a material can be understood. Hysteresis results in heat dissipation with the area of the energy being proportional to the area of the magnetic hysteresis loop [16]. This leads to the concept of constant flow of energy into that material when you apply a time varying magnetic field to that ferromagnetic material. This is the physics basis of hyperthermia treatment [18]. The shape of the loop is partly determined by the particle size. Particles at the nano-scale exhibits superparamagnetism [18. The contribution of hysteresis loss differs depending on the size of the nano-particle **[**41].

When an external magnetic field is applied to a nano-particle, the magnetic moments align along the applied field.

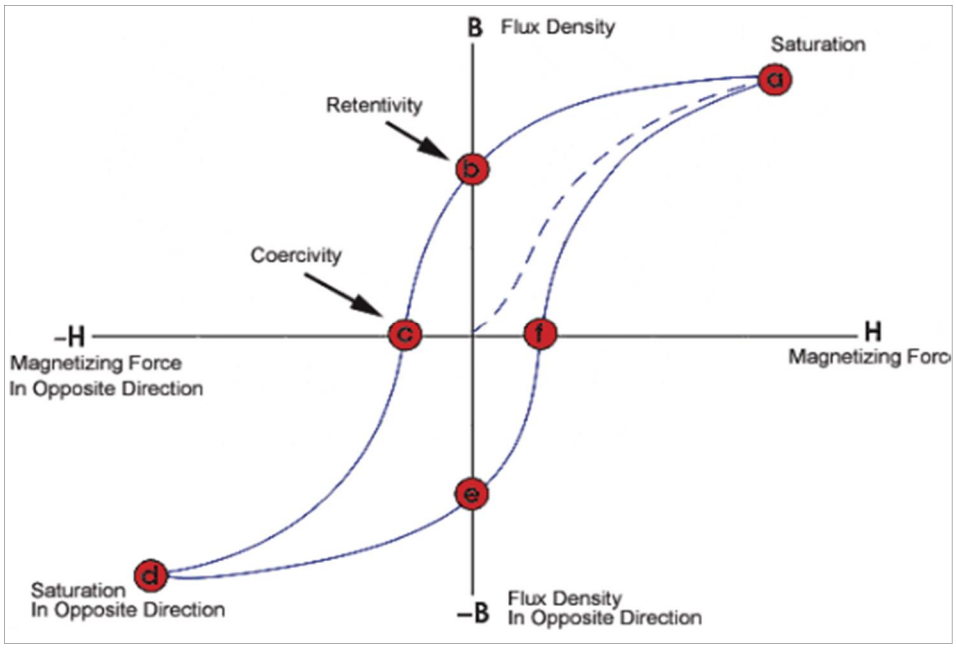

Figure 2.3: The response of a ferromagnetic material to applied magnetic field.

2.4 Magnetic Field

Magnetism is defined as the force produced by charge particles of a magnet. Every charged particle produced a magnetic field when it moves. For instance, the spinning of electrons in an atom generates a magnetic field around it. The magnetic Field strength of an electromagnet depends on the number of the turns of the coil and the current flowing through the coil as well as the type of material used. Higher field strength can lead to aggregation of magnetic materials which eventually lead to embolism [20]. Magnetic fields are used as external stimuli to control the behaviour of complex geometry of magnetic nanoparticles [23]. By moving a wire or changing a magnetic field, there is an induced voltage and current within the coil. This process is called electromagnetic induction [28].

2.4.1 Magnetic Materials

Magnetic materials under the influence of external magnetic field show different characteristics. Their response to the field is dependent upon temperature. When an external magnetic field is applied to a material, the magnetic moment of the electrons aligns themselves with the B so that the net magnetic field is not zero. The paramagnetic material is displayed by substances that have unpaired electrons in their atomic orbital. They have non-interacting spins that is characterised by linear susceptibility which is inversely dependent on the Curie temperature [64]. The ferromagnetic materials are characterised by exchange interactions, and hysteresis. They are composed of magnetic domains which points in random direction leading to a zero net magnetic moment. They retain their magnetic moment after the external filed is switched doff. By continuous reducing the size of the materials, the magnetization measured becomes zero, thus there is no coercivety in such a material and therefore, it behaves like a paramagnetic or superparamagnetic nanoparticle.

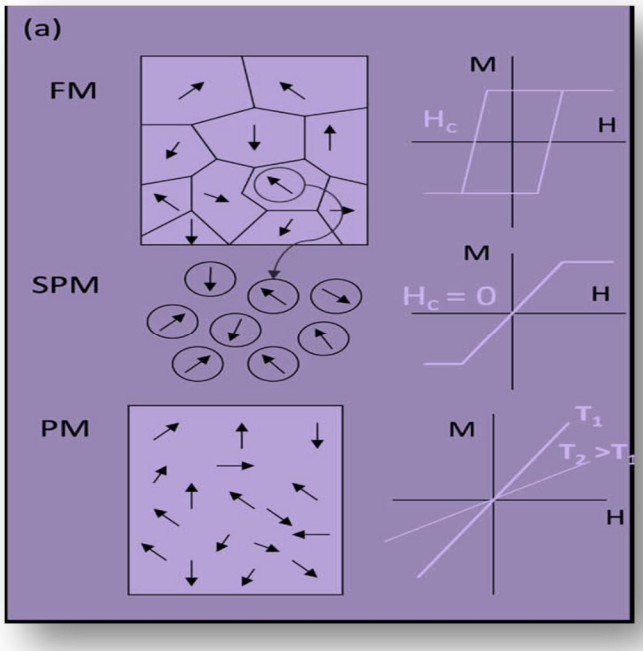

Figure 2.4 : Magnetic materials showing different magnetic behaviour

2.4.2 Basic Concepts of Magnetic Field

If a material is placed in a magnetic field of strength, H, there is a magnetic induction [18].

$$B = \mu_O(H + M) \quad (2.2)$$

Where

μ_o is the permeability of free space, $M = \frac{m}{v}$ Is the magnetic moment per unit

In terms of volumetric magnetic susceptibility,

$$M = \chi H \quad (2.3)$$

Where

χ is the magnetic susceptibility

The magnetic field generated by a steady current I is described by the Biot- Savart Law [26].

$$B = \frac{\mu_o I}{4\pi} \int \frac{\hat{r}}{r^2} dl \quad (2.4)$$

Where

μ_o is the magnetic constant

r is the distance between the location of dl and the location at which the magnetic field is calculated, $\hat{r}$Is a unit vector in the direction of r. A more general way of relating the current I to the B-field is through the Ampere's law [27].

$$\oint B.dl = \mu_o I_{enc} \quad (2.5)$$

The ampere's law describes the fact that an electric current can generate an induced magnetic field. In a stable magnetic field, the integration along a magnetic loop is equal to the electric current the loop encloses

$$\oint H.dl = j \quad (2.6)$$

Where H is the magnetic field,

I is the current 11

We recall that curl of a vector

$$curl\ A = \nabla xA \lim_{\Delta s \to 0} \frac{\oint A.dl}{\Delta s} n \tag{2.7}$$

Replacing A by H

$$Curl\ H = \nabla xH = \lim_{\Delta \to 0} \frac{\oint_L H.dl}{\Delta s} n = \frac{j}{\Delta s} = J \tag{2.8}$$

j is the current density in an infinitesimal area

For a varying electric field with respect to time;

$$\nabla xH = J + \frac{\partial D}{\partial t} \tag{2.9}$$

Faraday's law states that a moving magnet can generate an alternating electric field. The moving magnet can be represented by the variation of vector magnetic potential ψ

$$E = -\frac{\partial \psi}{\partial t} \tag{2.10}$$

Taking cross product

$$\nabla xE = -\nabla x \frac{\partial \psi}{\partial t} = \frac{-\partial}{\partial t}(\nabla x \psi) \tag{2.11}$$

$$\nabla xE = \frac{-\partial B}{\partial t} \tag{2.12}$$

Applying the Gaussian theorem which states that the integration of the divergence of a vector field over a certain volume is equivalent to the vector field itself integrated over the entire closed surface that contains the volume

$$\int_v \nabla . A dv = \int_s A . ds \tag{2.13}$$

$$D = \in E \tag{2.14}$$

$$E = \frac{qr}{4\pi \in r^3} \tag{2.15}$$

Applying the div theorem,

$$\nabla . D = \lim_{v \to 0} \int_s D . ds = \lim_{v \to 0} \int_s \in E . ds = \lim_{v \to 0} \int_s \in \frac{qr}{4\pi \in r^3} ds \tag{2.16}$$

$\nabla . \mathrm{D} = \frac{\mathrm{q}}{\mathrm{v}} = \rho_e$

ρ_e is the charge density in the infinitesimal volume confined by the enclosed surface. The Maxwell equations governing the electromagnetic field are;

$$\nabla x\, H = J + \frac{\partial D}{\partial t}$$

$$\nabla x\, E = -\frac{\partial B}{\partial t}$$

$$\nabla . B = 0$$

$$\nabla . D = \rho_e$$

2.4.3 Magnetic Induction

Finding the magnetic field everywhere around the hemozoin. As the field oscillate in cyclic form, they cause the hemozoin to spin around in a circular form. We can therefore calculate the magnetic induction inside the parasite. The cross-section area is given by

πa^2

Using the integral form of the Ampere's law, we can find the magnetic induction

$$\oint B . d\vec{l}_1 = \mu_o \int \vec{J}\ \hat{n}\ da$$

$$B\phi . 2\pi\rho = \mu_o \int \frac{I}{A} . da$$

$$B\phi . 2\pi\rho = \frac{\mu_0 I}{A} \int da$$

$$B\phi . 2\pi\rho = \frac{\mu_o I}{A} [a]_b^\rho$$

$$B\phi . 2\pi\rho = \frac{\mu_o I}{A} (\pi\rho^2)$$

$$B\phi = \frac{\mu_{OI\rho}}{2\pi a^2}$$

2.4.5 Force in Magnetic Field

The magnetic field is most commonly defined in terms of the Lorentz force it exerts on moving electric charges. A particle moving in a magnetic field experiences a force that is proportional to the strength of the field. This is the Lorentz force:

$$F = qv \times B \tag{2.18}$$

Where

q is the electric charge, v is the instantaneous velocity of the particle

B is the magnetic field

2.4.6. Consequence of Magnetic Force

The magnetic force points perpendicular to the charges velocity. Therefore finding the radius of motion [29]

$$F_{mag} = F_{centripetal} \tag{2.19}$$

$$F_{mag} = \frac{q\,v\,B}{c} \tag{2.20}$$

$$F_{centripetal} = \frac{mv^2}{R} \tag{2.21}$$

$$R = \frac{mvc}{qB} \tag{2.22}$$

Magnetic force does not work on moving charge [30].

$$dW = \vec{F}.d\vec{s} = \vec{F}.\vec{v}dt \tag{2.23}$$

$$dW = q\left(\frac{\vec{v}}{c} \times \vec{B}\right).\vec{v}dt \tag{2.24}$$

$$dW = 0 \tag{2.25}$$

This implies that the magnetic field is perpendicular to the velocity $\vec{v} \times \vec{B}$

For a particle moving in a given electromagnetic field, there are two actions acting on it;

The action of the free particle, and the term describing the interaction of the particle with the field [30]. A charge located in the field is not only subjected to external force by the field but also in turns act on the field. Finding the equation of motion of a charge in an electromagnetic filed;

$$\frac{\mathrm{d}}{\mathrm{dt}}\left(\frac{\partial \mathrm{L}}{\partial \mathrm{v}}\right) = \frac{\partial \mathrm{L}}{\partial \mathrm{r}} \tag{2.27}$$

$$\mathrm{L} = -\mathrm{mc}^2\sqrt{1-\frac{\mathrm{v}^2}{\mathrm{c}^2}} + \frac{\mathrm{e}}{\mathrm{c}}\mathrm{A}.\mathrm{v} - \mathrm{e}\phi \tag{2.28}$$

The integrand is the Lagrangian for a charge in an electromagnetic field, $\frac{e}{c}A.v - e\phi$ Describe the interaction of the charges with the field ,$\frac{\partial L}{\partial v}$ Is the generalizes momentum of the particle

2.5 Magnetic Particle

When soft magnetic structure is placed in a homogeneous magnetic field, it concentrates the field which induces elevation of the field strength. In effect, it introduces a field gradient which directs the movement of the magnetic particle [21]. Magnetic nanoparticle obeys the coulomb's law and therefore, they can be manipulated by external magnetic field gradient [24]. Small particle sizes have comparatively high surface immobilized molecules [22].

A randomly magnetized object has dipole approximation when they are far apart [23]. This enables their interactions energy to be computed. In recent years, chains of magnetic nanoparticles are of great importance in the medical application of ferro-fluids [24].

2.5.1 Effect of heat on magnetic nanoparticle

When magnetic nanoparticles are subjected to electric current, the current causes the MNPs to spin about their moment which eventually lead to their death. These magnetic nanoparticles possess super paramagnetic property as a result of exposure to AC [23]. Magnetic materials under the influence of AC are convenient for hyperthermia application [20]. Rosensweig gave detailed information based on Debye model for dielectric dispersion in polar fluids on the heating process for the magnetic nanoparticle. Application of an alternating magnetic field to a magnetic nanoparticle makes the magnetic moment of the MNP to rotate and align with the changing filed [25].

Chapter Three

3.1 Cyclic Electromagnetic Field

One such advantage of using cyclic electromagnetic filed is that the field increases the sensitivity of the parasite to low concentration of anti-malarial drugs and, therefore enhances the effective treatment of the disease [31]. The oscillating magnetic field may affect the parasites in two ways, according to Lai. In organisms still in the process of binding free heme molecules into a large number, the field causes the stacked heme molecules to shake thus preventing more stacking. The oscillating field also causes the stacks to spin, which cause damage and death of the parasite [31].

Systems undergoing resonance are often used to generate vibrations at specific frequencies. As the parasites oscillate there is also an effect that tends to reduce the amplitude of the oscillation. This effect is known as damping, which is as a result of some losses from cycle to cycle. This oscillation causes vibrations in all direction between the parasites which effectively result in collision and eventually leads to the generation of heat. As the particles collide with each other, they gain momentum and are able to travel past their mean position [32]. For forced vibrations, the parasites are driven at constant amplitude and the energy per cycle is given by [33]:

$$\partial w = 2u\delta \tag{3.1}$$

Where,

∂w is the hysteresis loop area (See figure 2.1), 2u is the total energy per cycle, δ is the internal friction

3.1.2 Heat Generation

When an oscillating magnetic field is applied to the malaria parasite, the oscillation of the field results in heat generation. The heat generation is due to the collision of the particles inside the hemozoin. Therefore, according to Lai, treating over 5oo million people every year who are infected with malaria using oscillating magnetic field would be inexpensive and very simple **[**31].

The heat equation (Fourier's law) is given by;

$$\frac{du}{dt} = \alpha \frac{d^2u}{dx^2} \quad (3.2)$$

Where

u is the temperature gradient, α is the thermal diffusivity, which is given by;

$$\alpha = \frac{k}{c_p}\rho \quad (3.3)$$

Equation 3.2 describes the evolution of temperature within a finite one dimensional medium with no internal heat source. In order for us to determine the temperature, we decided to specify the temperature distribution along our system at an initial condition.

Assuming an adiabatic system in which there is no heat transmitted through the surface and on the system, a finite difference scheme of forward, backward and central difference approximations was used to estimate the temperature gradients within the plane.

The finite difference scheme was use to obtain numeral solutions to the heat equation. In using the numerical solution, the particle differential equation, in the heat equation is replaced with discrete approximations. Therefore, in the physical domain, the solutions are known only at finite number of points.

3.2 Models

In order to achieve the analytical models of the hemozoin, we assumed the cyclic behaviour of the electromagnetic field to be a harmonic oscillating field. This is because the hemozoin exists as a crystalline structure in a fluid inside of the membrane. For a lightly damped a linear oscillator, with resonance frequency, Ω, the intensity of oscillation, I, when the system is driven with a frequency , ω ,is typically approximated by the following expression that is systemic about the resonance frequency [34];

$$I(\omega) = \frac{(\Gamma/2)}{(\omega-\Omega)^2+(\Gamma/2)^2} \quad (3.4)$$

Γ is the parameter dependent on the damping of the oscillator and is known as the line-width of the resonance. The line-width is inversely proportional to the Q factor, which is a measure of the

sharpness of the resonance. Oscillators with high quality factors have low damping so they ring longer, The Q factor, is given by;

$$Q = 2\pi x \frac{Energy\ Stored}{Energy\ loss\ per\ cycle} \tag{3.5}$$

The equation of a damped harmonic oscillator is given by;

$$\ddot{x} + c\frac{\dot{x}}{m} + k\frac{x}{m} = 0 \tag{3.6}$$

$$\frac{d^2x}{dt^2} + 2\zeta\omega_o \frac{dx}{dt} + \omega_0^2 x = 0 \tag{3.7}$$

Where the natural frequency, ω_0, is given by;

$$\omega_0 = \sqrt{\frac{k}{m}} \tag{3.8}$$

and the damping coefficient is expressed as;

$$\zeta = \frac{c}{2\sqrt{mk}} \tag{3.9}$$

Equation in 3.7 yields different types of behaviour for different parameter values and the amplitude that the oscillator eventually acquires depends on the relation of the driving frequency to the natural frequency of the oscillator and it also depends on the damping factor.

The analytical solution to equation 3.4 is;

$$x(t) = Ae^{\alpha t} + Be^{-\alpha t} \tag{3.10}$$

Combined with real experimental data, the solutions to equation 3.10 can be used to determine whether the forcing frequency can induce resonance or not [35].

3.2.1 Analytical Method

In this section, the separation of variables method is used to solve the heat equation. We assume a homogeneous boundary condition, in that the system is kept at a prescribed temperature. Such a condition is called Dirichlet boundary condition. This gives:

$$u(t,0) = u(t,l) = 0 \tag{3.11}$$

Separation of variables in equation 3.2 gives us two ODEs in X, and T

$$u(x,t) = X(x)T(t) \tag{3.12}$$

$$X(x)T''(t) = \alpha X''(x)T(t) \tag{3.13}$$

$$\frac{T'(t)}{\alpha\, T(t)} = \frac{X''(x)}{X(x)} \tag{3.14}$$

Since x and t are independent variables, the only way they could be equal is when we equate both to a constant;

$$T'(t) = -\lambda\alpha T(t), \tag{3.15}$$

$$X''(x) = -\lambda X(x) \tag{3.16}$$

The general solution for the first part gives;

$$T(t) = ce^{-\lambda\alpha t} \tag{3.17}$$

Now, we find the solution for the second part in equation 3.16

$$X'' + \lambda X = 0 \text{ with } X(x) = X(l) = 0 \tag{3.18}$$

This is a two point boundary problem also known as Sturm-Liouville problem, we make some assumption,

$$\lambda<0, \tag{3.19}$$

$$X(x) = Ae^{\lambda x} + Be^{-\lambda x} \tag{3.20}$$

After plugging in the boundary conditions, we find that the constants, A and B are both zeros. We make another assumption.

$$\lambda=0 \tag{3.21}$$

The solution to equation (3.16) gives;

$$X(x) = ax + b \tag{3.22}$$

Again, a=b=0, and we arrive at zero solution.

Hence, we take the positive value of λ,

$\lambda > 0$ (3.23)

The general solution to equation (3.16) gives;

$X(x) = D\cos\lambda x + \sin\lambda x$ (3.24)

After applying the boundary condition,

$X(0) = 0$, meaning D=0 (3.25)

$X(l) = 0$, meaning $E\sin\lambda l = 0$ (3.26)

Since sine is equal to zero for positive value of π, therefore,

$\lambda_n = \frac{n^2\pi^2}{l^2}$ (3.27)

And E=1

$X_n = \sin\frac{n\pi x}{l}$ (3.28)

λ_n is the eigen value and X_n is the eigen function

The complete solution to the Sturm-Liouville problem is;

$U_n(x,t) = \sin\frac{n\pi x}{l}e^{-n^2\pi^2\alpha t}$ (3.29)

This equation 3.29 looks like a standing wave whose amplitude decays exponentially over time.

The solution to equation 3.12 is given by;

$u(x,t) = \sum_{n=i}^{+\infty} b_n \sin\frac{n\pi x}{l}e^{\frac{-n^2\pi^2\alpha t}{l^2}}$ (3.30)

$b_{n=\frac{2}{l}}\int_0^i f(x)\sin\frac{n\pi x}{l}d_x$ (3.31)

3.2.2 Numerical Method

Equation 3.2 was also solved using a Matlab R2007 code (Appendix). This was based on approximation with the forward Euler method. This gives;

$\frac{u_i^{k+1}-u_i^k}{\Delta t} = \alpha\left(\frac{u_{i-1}^{k+1}-2u_i^k+u_{i+1}^k}{h^2}\right)$ (3.16)

This is the first order in time and second order in space. In order to advanced more quickly, we chose to let $\Delta t = h$ (3.17)

For the finite difference scheme to work effectively we investigated the consistency and stability of the scheme and noticed that it was consistent since the limit of the truncation error is zero as h approaches zero. The truncation error was calculated by calculating the difference between the analytical results and the numerical estimates and a graph was obtained using Matlab.

Now applying a boundary condition for a two dimensional steady-state temperature distribution in finite approximation:

$$\frac{u_{i,j}^{k+1}-u_{i,j}^{k}}{\Delta t} = \alpha\left(\frac{u_{i,j+1}^{k}-2u_{i,j}^{k}+u_{i,j-1}^{k}}{\Delta x^2} + \frac{u_{i+1,j}^{k}-2u_{i,j}^{k}+u_{i-1}^{k}}{\Delta y^2}\right) \quad (3.18)$$

The boundary conditions are given by;

$u(x,0)=0; \quad 0<x<5$ (3.19)

$u(0,y)=0; \quad 0<y<10;$ (3.20)

$u(x,10) = 100\sin(\pi x/10), \; 0<x<5, \; \frac{\partial u(5,y)}{\partial x} = 0 \quad 0<y<10$ (3.21)

A quadrilateral mesh with one degree of freedom for each node, four numbers of elements and 25 elemental nodes was computed using Matlab.

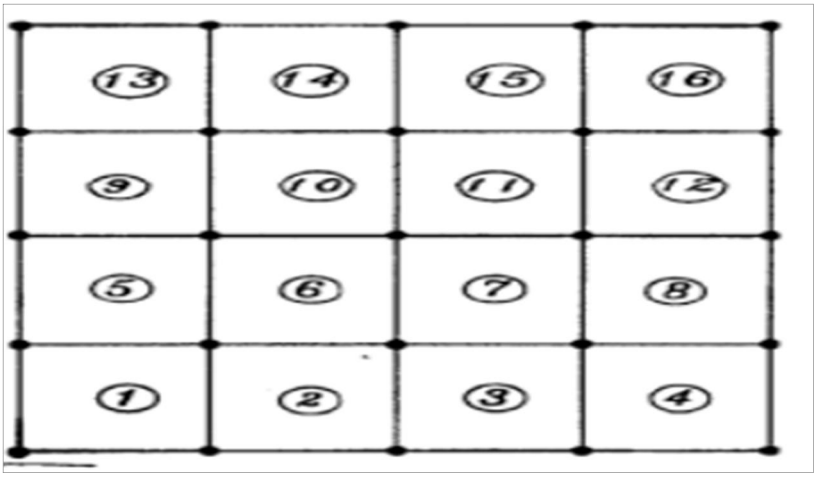

Figure 3.1; Schematic of Typical Rectangular Mesh used in Finite Difference Analysis

3.2.3 Analysis

The mesh is the set of locations where the discrete solution is computed and this point are called nodes. Decreasing the truncation error by using finer mesh may result in increasing the round-off error due to the increased number of arithmetic operations. It formation essentially removes the reactive iron of heme out of the solution where the haemoglobin degradation occur **[**36**]**. In general, increasing the number of nodal points not only increases the resolution but also the accuracy of the numerical solution. We used a smaller mesh size to increase accuracy of the finite difference simulations.

3.3 The Heme as Magnetic Nanoparticle

Ferritin is a ubiquitous intracellular iron storage found to be a hem binding protein [65]. The ferritin found in mosquito is a high molecular weight protein composed of several different, relatively small subunits [66]. Cavities formed by ferritin protein have been used as reaction chamber for fabrication of metallic nanoparticle [67]. It consists of an inorganic core of diameter 7nm and a protein shell of 6nm [69]. Ferritin contains antimagnetic ferrihydrite with relatively low magnetic moment at the core, but for applied purposes, the core is been replace by magnetite for higher magnetization [69]. The irons in the ferritin core are stored as Fe (III) in a crystalline solid, however, these irons are reduced from the Fe (III) oxidation stage to the Fe (II) oxidation state through a hydrolysis synthesis. The best model for ferritin core is the mineral ferrihydrite also called goethite; FeO (OH) [68].The morphology of ferrihydrite is spherical [72]. Goethite is present in iron nanoparticle as an admixture. The goethite nanoparticle has nonzero magnetic moment due to it incompatible compensation of the magnetic moment of the sublattice [69]. The magnetic nanoparticle depends on external factors such as temperature, pressure and in some case the medium in which the particles occurs, i.e. crystalline, or amorphous balk matrix [69]. Aqueous suspension of goethite nanorods are poly dispersed particle of about 150nm longs, 25nm wide and 10nm think. The suspension display a nematic phase at equilibrium in a well-defined concentration range. In order words, they exhibit magneto- orientational behavior in dilute suspension [73]. The magnetic field intensity required to align the nematic phase is 20mT

for a $20-\mu m$ [71].

3.3.1 Nanoparticle Heating

In this research, we considered the particles inside the heme as a magnetic nanoparticle. The formation of the hemozoin prevents oxygen radical-medicated damage to the malaria parasite. The oscillating field influences the heating of the nanoparticle. Magnetic nanoparticles generate heat under oscillating fields by physical mechanisms such as relaxation loss or hysteresis loss. These generally depend on the frequency of the field as well as the particle size.

Recent research has shown that magnetic nanoparticles with size of 5-200 nm can induce heat in biological systems at the molecular level [39]. Magnetic nanoparticles can be manipulated using a magnetic field. Their physical and chemical properties depend on their method of synthesis as well as their chemical structure [37]. In this research however, we focus on the ferrite nano-particles because Ferrite nanoparticles exhibit magnetic behaviour once an external magnetic field is applied to it [38]. Therefore, we anticipate that considering the particles inside the hemozoin as magnetic nanoparticles, they can be trapped inside, as external field is applied causing an induced heat and eventually make it inactive. The size and shape determines the response of the nanoparticle to the induced heat [40]. The rate of heat dissipation of nanoparticle is inversely related to the particle size, Hence small particle size should enhance the level of heating.

The thermodynamics of the heated particle can be modelled using the first law of thermodynamics. This gives;

$$dU = \partial Q + \partial W \tag{3.22}$$

where

U is the internal energy, Q is the heat added to the system and W is the work done by the system. From this equation, we can determine the energy produced as a result of the oscillation of the field. In any case, if we consider our system such that, there is no heat transfer between the system and the surrounding environment, then the net heat transfer to or from the system is zero, i.e. Q = 0. This implies that the internal heat energy, which is an extensive property, equals the work done by the system undergoing the adiabatic process.

$$dU = \partial W \tag{3.23}$$

For differential work give in-terms of magnetization,

$$\partial W = H.dB \tag{3.24}$$

For collinear field in which the magnetization density is treated as a vector field and not as a scalar field,

$$dU = H.dB \tag{3.25}$$

This reduces to

$$dU = HdB \tag{3.26}$$

H which is the magnetic field intensity is measured in Am^{-1}. While, the magnetization induction is measured in Tesla

$$B = \mu_o(H + M) \tag{3.27}$$

Where μ_o is the permeability of free space, Hence substituting, we get

$$du = H.d[\mu_o(H + M)] \tag{3.28}$$

$$du = \mu_o[H.d(H + M)] \tag{3.29}$$

After performing cyclic integration, we obtained

$$\Delta u = -\mu_o \oint MdH \tag{3.30}$$

This is the internal energy dissipated in one cycle during hysteresis which leads to heating.

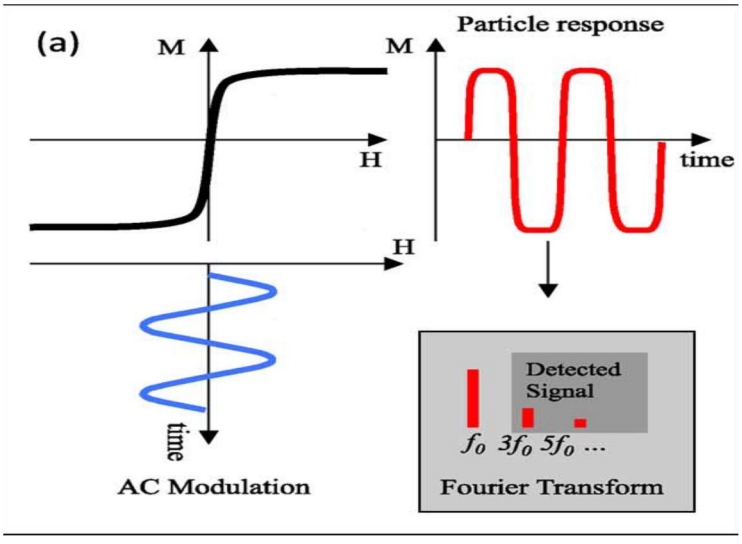

Figure 3.2: Response of magnetic particle to external magnetic field.

The magnetization curve, as a function of the applied field, is a reversible S-shaped function. If we make the assumption that all the hemozoin particles are identical implying that they have the same energy barrier and same magnetic moment, then we can express the magnetization as

$$M(H) = n\mu \tan h\left(\frac{\mu_o H \mu}{k_B T}\right) \quad (3.31)$$

Where

n in the density of nanoparticles , μ_O is the magnetic permeability, μ is the magnetic moment of nanoparticle.

In terms of volumetric magnetic susceptibility of the magnetic nanoparticles;

$$M = \chi H, \quad (3.32)$$

χ is the magnetic susceptibility, which can also be expressed in the complex form as

$$\chi = \chi^{I} - i\chi^{II} \quad (3.33)$$

For a time varying magnetic field of amplitudeH_O;

$$H(t) = H_o cos\omega t \quad (3.34)$$

And magnetization of;

$$M(t) = H_o(\chi^{I} cos\omega t + \chi^{II} sin\omega t) \quad (3.35)$$

Subtitling equation 3.34 and 3.35 into equation 3.30 gives

$$\Delta U = \mu_o H_o^2 \int_0^{\frac{2\pi}{\omega}} (\chi^{I} cos\omega t + \chi^{II} sin\omega t) sin\omega t \, dt \quad (3.36)$$

$$\Delta U = \mu_o H_o^2 \left[\chi^{I} \int_0^{\frac{2\pi}{\omega}} cos\omega t \, sin\omega t \, dt + \chi^{II} \int_0^{\frac{2\pi}{\omega}} sin^2\omega t \, dt\right] \quad (3.37)$$

After performing this integration, we get;

$$\Delta U = 2\mu_o H_o^2 \int_0^{\frac{2\pi}{\omega}} sin^2\omega t \, dt \quad (3.38)$$

The factor 2 is as a result of the integration over the entire space ($-\infty$ to $+\infty$)

3.3.2 Mechanism

One mechanism by which the nanoparticle can generate heat is considering the relaxation losses on single-domain magnetic particles which fall under Brownian rotation or Neel mode [63]. In the latter mode, the particles are not allowed to move randomly within the sample but the movement is restricted only to the core of the particle [61.63]. This does not allow maximum heating rate to be achieved [25]. However, in the Brownian mode, the entire particle rotates in the fluid. It expression is given by;

$$\tau_B = \frac{3\eta V_H}{KT} \tag{3.39}$$

η is the viscosity coefficient , K is the Boltzmann constant, T is the absolute temperature(K), V_H is the hydrodynamic volume of the particle which is larger than the magnetic volume given by $V_M = \frac{4\pi R^3}{3}$ for a particle with radius R, $V_H = \left(\frac{1+\delta}{R}\right)^3 V_M$, δ is the thickness of the sorbed surfactant layer

However, since the particles are moving randomly with the sample, it becomes difficult to locate each particle at a given step.

$$\underline{R} = \sum_{i=1}^{N} \hat{b_i}\, b_o \tag{3.40}$$

Where $\underline{b_i}$ is a unit vector of length of b_o . Since all the steps are uncorrected

$$\|\underline{R}\| = \sum_{i=1}^{N} b_o \|b_i\| = 0 \tag{3.41}$$

The expression for the Neel mode is given by;

$$\tau_N = \frac{\sqrt{\pi}}{2}\tau_o \frac{\exp(KV/K_B T)}{(KV/K_B T)^{\frac{1}{2}}} \tag{3.42}$$

K is the anisotropy constant; V is the volume of the particle and $K_B T$ is the thermal energy. The weighted average between the Ne'el and the Brownian relaxation is the effective relaxation given by;

$$\frac{1}{\tau} = \frac{1}{\tau_N} + \frac{1}{\tau_B} \tag{3.43}$$

3.3.3 Power Dissipation

Rotation of particle results in Brownian mechanism of relaxation as well as the N´eel relaxation in which the magnetic moment rotates within the crystal [25]. Both mechanisms however, results in power dissipation due to friction [20]. The volumetric power dissipation due to the magnetic workdone on a system in an adiabatic process is given by [25, 61] is

$$p = f\Delta u = \mu_o \pi \chi^{II} f H_o^2 \tag{3.44}$$

Where

χ^{II} is the magnetic susceptibility function, f is the frequency of the AC magnetic field, H_o is the magnitude of the applied magnetic field. Heat generation for magnetic fluid is expressed as[20]

$$\text{SAR X Particles density} = p$$

Where

SAR is the specific absorption rat which is the heat power release per gram of magnetic material upon ac-field application.

$$SAR = \frac{\mu_o \pi \chi^{II} f H_o^2}{\rho} \tag{3.45}$$

where ρ is the mass density of the magnetic nanoparticle, χ_o is the equilibrium susceptibility and τ is the effective relaxation time [61].

The relaxation equation for a fluid in oscillator field is expressed as;

$$\frac{\partial M(t)}{\partial t} = \frac{1}{\tau}[M_o(t) - M(t)] \tag{3.46}$$

$$M_o = \chi_o H_o \cos\omega t = Re\left[\chi_o H_o e^{i\omega t}\right], \quad M(t) = Re\left[\chi H_o e^{i\omega t}\right] \tag{3.47}$$

After performing the differentiation, we obtained

$$\chi = \frac{\chi_o}{1+i\omega\tau} \quad (3.48)$$

Equation in 3.49 gives the expression for the susceptibility and it dependences on frequency [25]

$$\chi^{II} = \frac{\chi_o \omega\tau}{(1+(\tau\omega)^2)} \quad (3.49)$$

$$\omega = 2\pi f \quad (3.50)$$

Substituting 3.49 and 3.50 into 3.51 gives the energy dissipation density for monodispersion [61] as

$$p = \mu_o \pi f \chi_o H_o^2 \frac{2\pi f\tau}{[1+(2\pi f\tau)^2]} \quad (3.51)$$

The equilibrium susceptibility χ_o of isotropic materials is described using the langevin equation; $L(\aleph) = \frac{M}{M_s} = \text{cth}\aleph - \frac{1}{\aleph}$, with $M_s = \phi M_d$ as the saturation magnetization of the aqueous medium, M_d is the domain magnetization of the suspended particle, ϕ is the volume fraction solid given by (0.05). $\aleph = \frac{\mu_o M_d H V_m}{KT}$, the initial susceptibility,

$$\chi_i = \frac{\mu_o V_m \phi M_d^2}{3KT}, \quad (3.52)$$

$$\chi_o = \chi_i \frac{3}{\aleph}\left(\text{cth}\aleph - \frac{1}{\aleph}\right) \quad (3.53)$$

The temperature rise is given as;

$$\Delta T = \frac{P\Delta t}{c} \quad (3.54)$$

Where, Δt is the duration of the heating, c is the specific heat capacity of the aqueous suspension of the goethite

3.4 Effect of Temperature and Pressure on Heme

Pressure is a thermodynamic property which increases with temperature increase. Mathematically, it can be expressed using the Gay- Lusssc's law as;

$$\frac{P}{T} = k \quad (3.55)$$

As temperature is increase, a number of bonds in the protein molecules become weaken. As heating continues, some of the cooperative hydrogen bonds that stabilizes the helical structure begins to break.

$$PV = kNT \quad (3.56)$$

K is the Boltzmann constant ($1.38\,x\,10^{-23}JK^{-1}$), N is the number of molecules. Exposure of most protein results in an irreversible denaturation. The Optimum temperature for Plasmodium falciparum protein (**Pfsd**) to survive in either host is between T_{min} (25.3°C) to T_{max}(33°C). However, the parasite loss its activity at $T_{min} \leq 7^0c$ and $T_{max} \geq 42^0c$ [73].

Studies have shown that electronic excitation energy is sensitive to a pressure range of 1 – 2 MPa [59]. Higher pressure in the range of 0.1- 0.5 GPa also distorts the secondary structure of electron in a reversible way [60]. At this pressure, the intermolecular interactions are also affected [Silva and Weber, 1988; Smeller et al., 1999]. Denaturizing of protein occurs at a pressure range of 0.5 – 1GPa [61]. Therefore, from this analysis, the denaturation phase diagram of protein can be determined.

From thermodynamic, we can find the energy gained by the particle is be equal to the applied force multiplied by the displacement of the particle.

$$\partial W = PdV \tag{3.57}$$

$$dU = -PdV \tag{3.58}$$

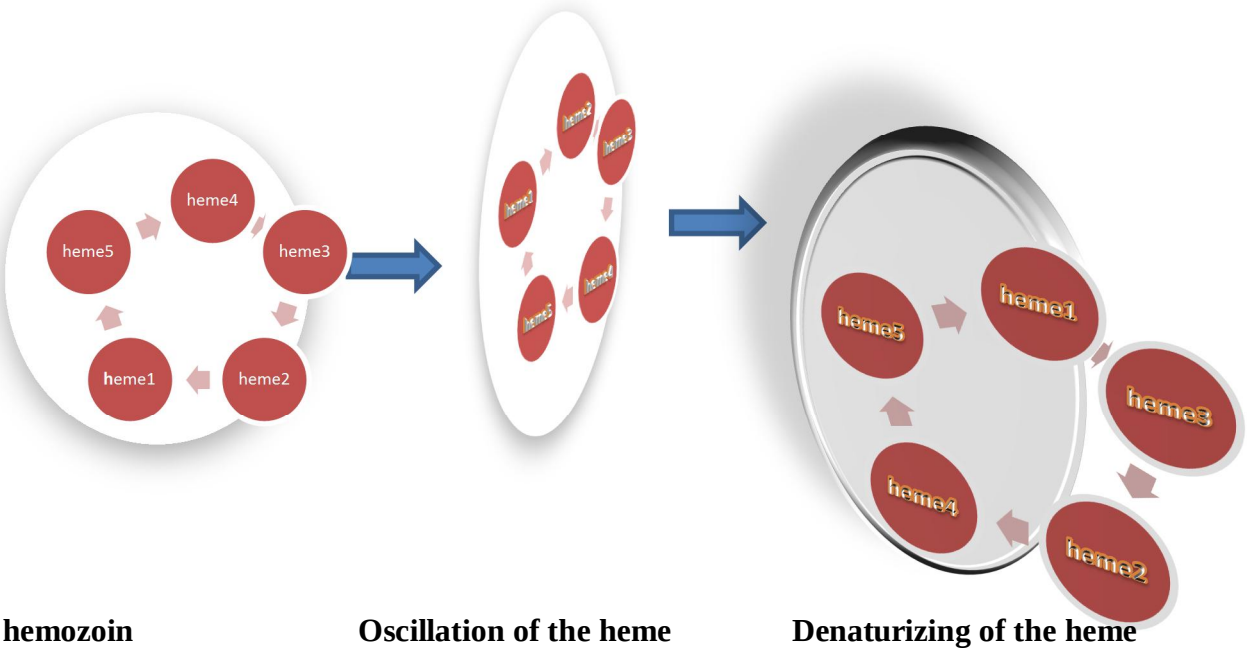

The hemozoin **Oscillation of the heme** **Denaturizing of the heme**

Figure 3.3: The effect of temperature and stress on the hemozoin as a result of oscillation of the Field and the heat generated

Given that the temperature of the sample increase as a results of its own heat dissipation, we can calculate the $\Delta T = T_2 - T_1$ by extrapolating the temperature drifts before and after the application of the field.

3.4.1 Effect of pH on hemzoin

As the reaction moves away from the optimal pH of 4, the percentage of heme conversion reduces. Below pH of 2, both propionic acid group are un-ionized and hemozoin formation is abolished, likewise at a pH (<6)

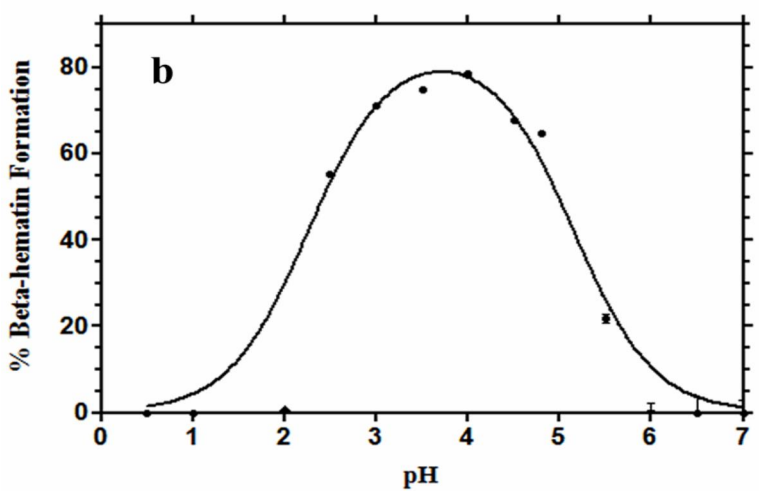

Figure 3.4 : The effect of pH was measured at 37 °C .The solid line fitted through the pH data is a best fit to an equation representing two pKa values with, pKa1 = 2.3 and pKa2 = 5.2

3.5 Molecular Diffusion:

An experiment conducted by Lauren M. et al reveals that, an increase in heat generated also increase the concentration of the MNPs. In this regard, we can use mathematical formation to validate this conclusion. We can find the concentration of N number of the MNPs with regards to the heat generated in a field of volume V.

$$\int d^3x(\partial_t c) + \int \underline{J}.ds = 0 \qquad (3.59)$$

Using divergence theorem,

$$\int d^3x \left(\partial_t c + \underline{\nabla}.\underline{J}\right) = 0 \quad (3.60)$$

$\partial_t c + \nabla . J = 0$ This is the conservation law. (3.61)

Considering Fick's law which relate the diffusive flux to the concentration by postulating that flux goes from a region of high concentration to a region of low concentration,

$$\underline{J} = -D\underline{\nabla} c \quad (3.62)$$

$$\partial_t c = D\nabla^2 c \quad (3.63)$$

Applying Initial and boundary conditions

$$c(x,t) = 0 \quad (3.64)$$

$$\underline{\nabla} c \to 0 \quad (3.65)$$

$$\underline{x} \to \infty \quad (3.66)$$

We can solve this using Fourier transform:

$$c(x.t) = \int \frac{d^2q}{(2\pi)^2} e^{-iq.x}\, c(q,t) \quad (3.67)$$

$$\partial_t c \int \frac{d^2q}{(2\pi)^2} e^{-iq.x} \partial_t c(q,t) = D\nabla^2 \int \frac{d^2q}{(2\pi)^2} e^{-iq.x}\, c(q,t) \quad (3.68)$$

$$\int \frac{d^2q}{(2\pi)^2} e^{-iq.x} \partial_t c(q,t) = -D\mathrm{q}^2 \int \frac{d^2q}{(2\pi)^2} e^{-iq.x}\, c(q,t) \quad (3.69)$$

Dividing through by

$$\int \frac{d^2q}{(2\pi)^2} e^{-iq.x} \quad (3.70)$$

$$\partial_t c(q,t) = -Dq^2 c(q,t) \quad (3.71)$$

$$\ln c\,(q,t) = -Dq^2 t + \ln k \quad (3.72)$$

$$c(q,t) = c(q,0) e^{-Dq^2 t} \quad (3.73)$$

$$c(q,0) = \int d^2x e^{iq.x} c(x,0) \quad (3.74)$$

$$c(q,0) = \int d^2x e^{iq.x}\, N\delta\left(\underline{x} - \underline{x_o}\right) \quad (3.75)$$

$$c(q,t) = Ne^{iq.\underline{x_o} - Dq^2} \quad (3.78)$$

Substituting it back to the Fourier series and completing the square, we obtain the concentration of the parasite as

$$c(\underline{x},t) = N\int \frac{d^2q}{(2\pi)^2} e^{-Dtq^2 - iq(x-x_o)} \quad (3.79)$$

$$c(x,t) = \left(\frac{N}{4\pi Dt}\right) e^{\frac{-(x-x_o)^2}{4Dt}} \quad (3.80)$$

3.6 Force of Attraction

Application of magnetic field generate a directional force on each magnetic per cycle. Since the malaria parasites have devolved resistance to drugs, there is also the tendency that they might also be resistant to the field. As a result, we calculate the force of attraction or repulsion between the hemozoin and the field.

$$\bar{F}_{12} = \frac{\mu_o I_1 I_2}{4\pi} \iint \frac{x_{12}}{(x_{12})^3} (dl_1 . dl_2) \quad (3.81)$$

From the diagram:

$$dl_1 = \widehat{ez} dz_1 \quad (3.82)$$

$$x_1 = z_1 ez \quad (3.83)$$

$$\widehat{ex} + z_2 \widehat{ez} \quad (3.84)$$

$$x_2 = c \quad (3.85)$$

$$\hat{e}x + (z_2 - z_1)\hat{e}z \quad (3.86)$$

$$x_{12} = x_2 - x_1 = c \quad (3.87)$$

$$x_3 = (c + a)\hat{e}x + z_3 \hat{e}z \quad (3.89)$$

$$x_{13} = x_3 - x_1 \quad (3.90)$$

$$x_{13} = (c + a)\hat{e}x + (z_3 + z_1)\hat{e}z \quad (3.91)$$

The loop consist of four sides but there is no contribution from sides (4) and (5) on the field. The two sides are perpendicular to the field, hence the angel between is 90.

$$dl_2 = \hat{e}z(-dz_2) = \hat{e}zdz_2 \tag{3.92}$$

$$\bar{F}_L = \frac{\mu_o I_1 I_2}{4\pi}\left[\iint \frac{x_{12}}{\|x_{12}\|^3}(dl_1.dl_2) + \iint \frac{x_{13}}{\|x_{13}\|^3}(dl_1.dl_3)\right] \tag{3.93}$$

$$\bar{F}_L = \frac{\mu_o I_1 I_2}{4\pi}[\iint \frac{c\hat{e}x+(z_2-z_1)\hat{e}z}{[c^2+(z-2-z_1)]^{3/2}}dz_1.dz_2 + \iint \frac{(c+a)\hat{e}x}{[(c+z)^2(z_3-z_1)^2]^{3/2}}dz_1.dz_3] \tag{3.94}$$

Separating these equations into two and solving them individually,

$$(A) = \iint \frac{c\hat{e}z+(z_2-z_1)}{[c^2+(z-2-z_1)^2]^{3/2}}(dz_1.dz_2) \tag{3.95}$$

We make changes of variables:

$$\xi_1 = z_2 - z_1,\ \ \xi_2 = z_2, \xi_1 = \xi_2 - \xi_1 \text{v} \tag{3.96}$$

$$dz_1 dz_2 = -d\xi_1 d\xi_2 \tag{3.97}$$

$$(A) = \iint \frac{(c\hat{e}x+\xi_1\hat{e}z)}{\left[c^2+\xi_1^2\right]^{3/2}}(-d\xi_1.d\xi_2) \tag{3.98}$$

Applying even and odd function and making change of variables:

$$(A) = \int \frac{c\hat{e}x}{\left(c^2\xi_1^2\right)^{3/2}}d\xi_1 \int \frac{c\hat{e}x}{\left(c^2\xi_1^2\right)^{3/2}}d\xi_2 \tag{3.99}$$

$$Let\ \xi_1 = ct, d\xi_1 = cdt, \tag{3.100}$$

$$\xi^2 = c^2t^2 \tag{3.101}$$

$$A = 2bc(c^2)\hat{e}x \tag{3.102}$$

Applying trigonometry function,

$$\text{Let } t = \tan\theta \tag{3.103}$$

$$dt = sec^2\theta d\theta = \frac{1}{cos^2\theta} \tag{3.104}$$

$$1 + t^2 = 1 + \frac{sin^2\theta}{cos^2\theta} \tag{3.105}$$

$$A = 2bc\hat{e}x \tag{3.106}$$

Going through the same procedure for the second part, we can find the total force on the field to be:

$$\bar{F}_L = \frac{\mu_o I_1 I_2 \hat{e}xba}{2\pi c(c+a)} \tag{3.107}$$

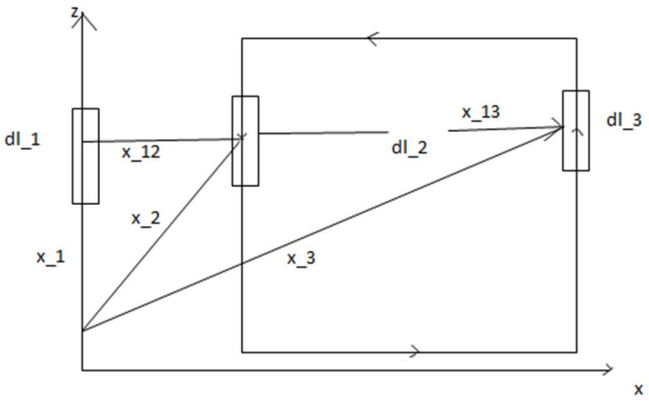

Figure 3.6: The directions of forces in the loop

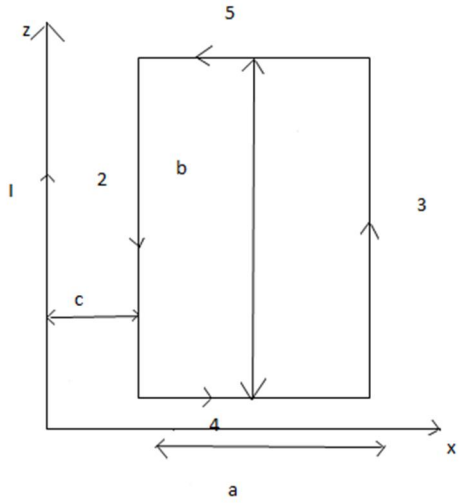

Figure 3.5: The forces in a magnetic loop

Chapter Four

4.1 Numerical Calculation on the Power Dissipation of Magnetic Field

In this study, we perform thermal analysis to predict the temperature distribution and the magnetic heating process for nanoparticle. From our numerical analysis, we noticed that, an increase in the frequency with a strong magnetic field causes heating of the magnetic nanoparticles. From the analytical calculation on the mechanism of heat dissipation, the temperature rise was s function of both the frequency and the magnetic field induction as well as the exposure time of the field. The range of magnetic field and frequency were chosen to be $0 < H < 15k$ A/m and $0.05 < f < 1.2$ MHz since higher or lower magnetic field could lead to the death of the mosquito. These values chosen were in accordance to the computational modeling of electromagnetic nanoparticle [70]. Experimentally, in a magnetic field induction of 0.3 T, the protein in the heme acquire enough energy to survive at a temperature of 24^{o}C with a frequency of 4.2 kHz and the volumetric power dissipated of 956.6890W/m^3 in 300 s window. Figure 4.5 below depict a graph of temperature against the exposure time of the field. A numerical simulation based on finite element scheme was employed to reaffirm this analysis. Figure 4.6 gives the temperature distribution within the mesh of the heme.

4.1.2 Comparison of experimental and simulation results of the survival of the parasite

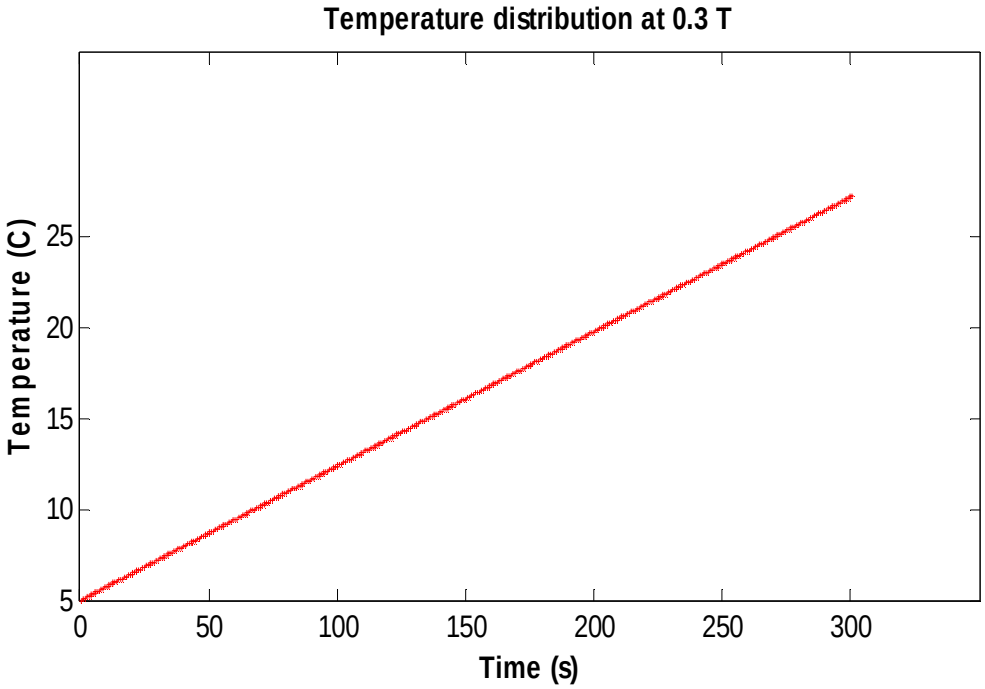

Figure 4.1: Experimental results of the amount of heat generated for a 0.3T at a frequency of 1.360 kHz. At a temperature of 24^{o}C, the particles acquire enough energy to survive

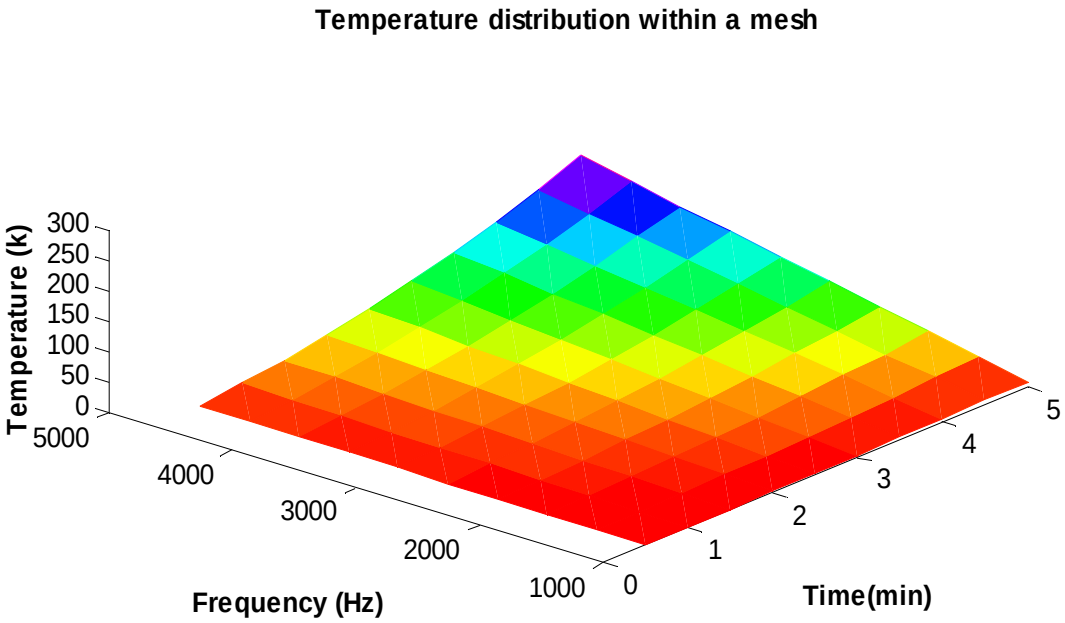

Figure 4.2 : A finite element discretization of the temperature distribution within each nodal point for the same time period of 300 s

4.1.3 Random nature of the particle within their body temperature

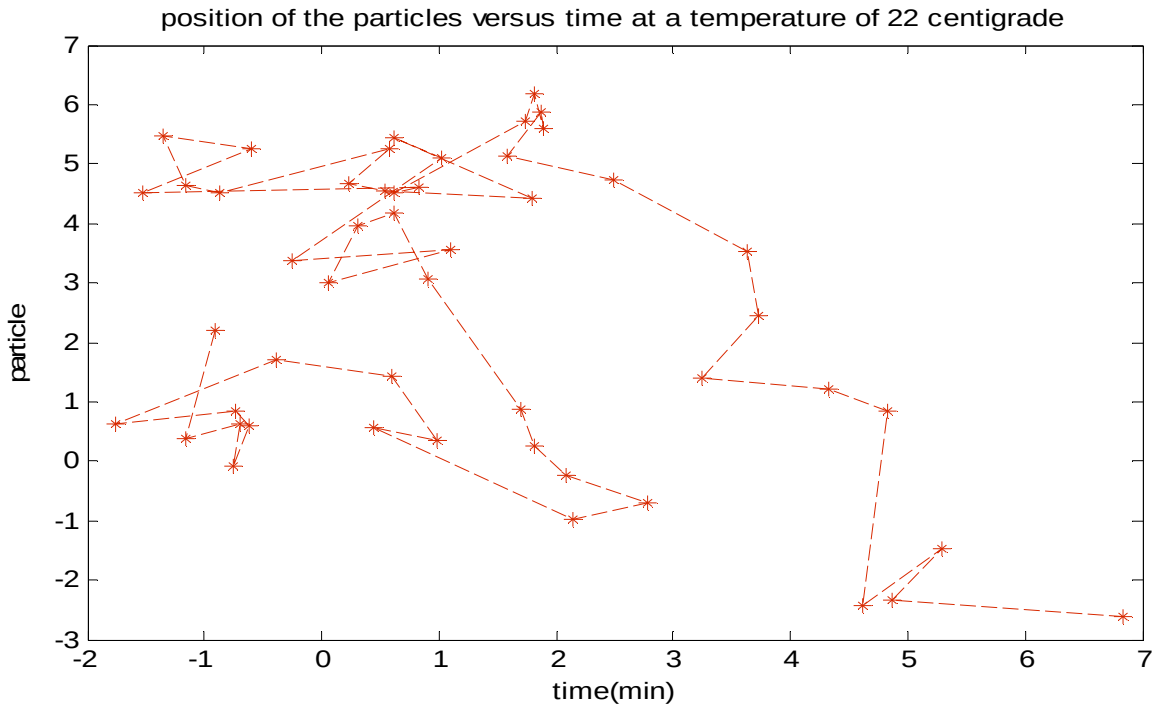

Figure 4.3 : A random distribution of the particle at field strength of 0.3T

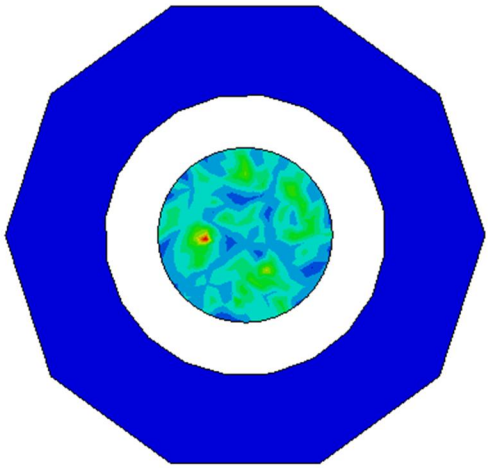

Figure 4.4 : Results of how the particles are randomly distributed within the medium

4.1.4 Molecular diffusion using Fick's law

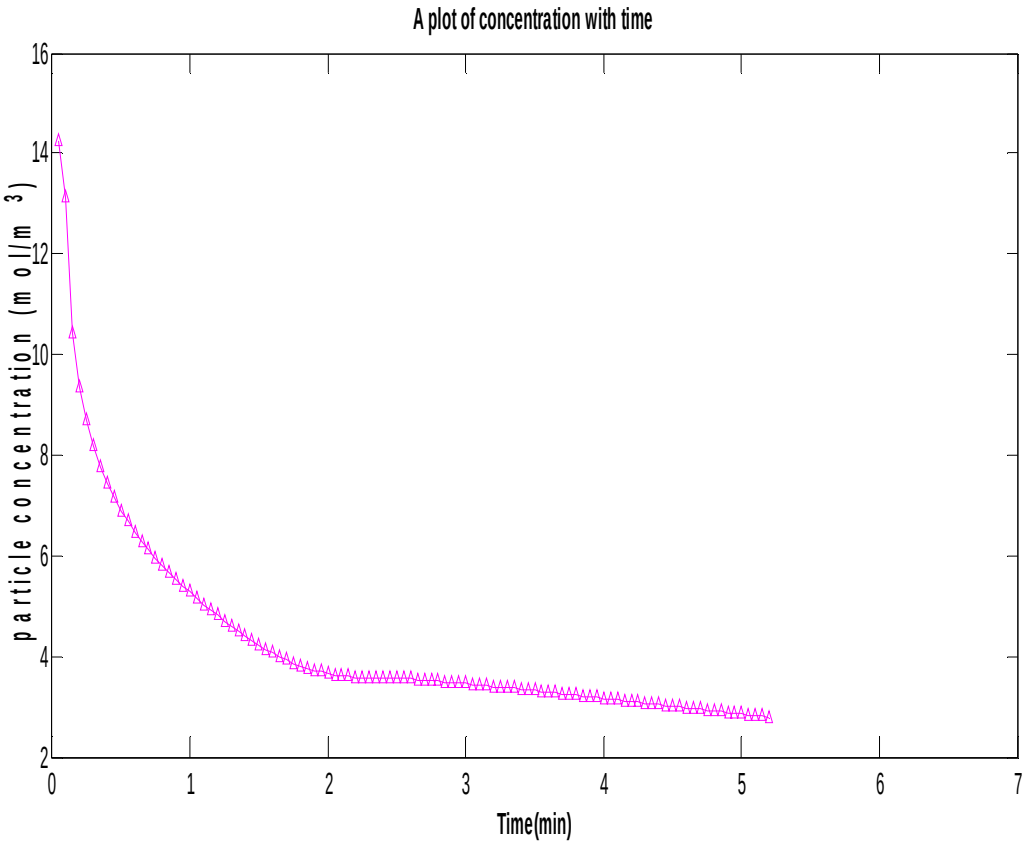

Figure 4.5 : The diffusion of particle from a region of high concentration to a region of low concentration with respect to time as the temperature is increased

4.5 Temperature rise of the Magnetic field for Higher Exposure Time

The amount of heat generated depends on the particle size, the amplitude of the field and the concentration of the nanoparticle. A nanoparticle of radius 4 nm and 5kA/m as the amplitude of field and effective relaxation time of $4.1303x10^{-11}s$ gave a temperature rise of 46^{o}C.

From our numerical simulation, at a higher exposure time of 900s, the temperature of protein also increase to 42^{o}C with an increase in the frequency to 4.6 kHz implying the longer the exposure time, the less active the parasite becomes since, they loss their activity at a higher temperature. The graph below shows both the experimental and the simulation result indicating the temperature increment with the frequency.

4.6 Membrane Rapture and heme Denature

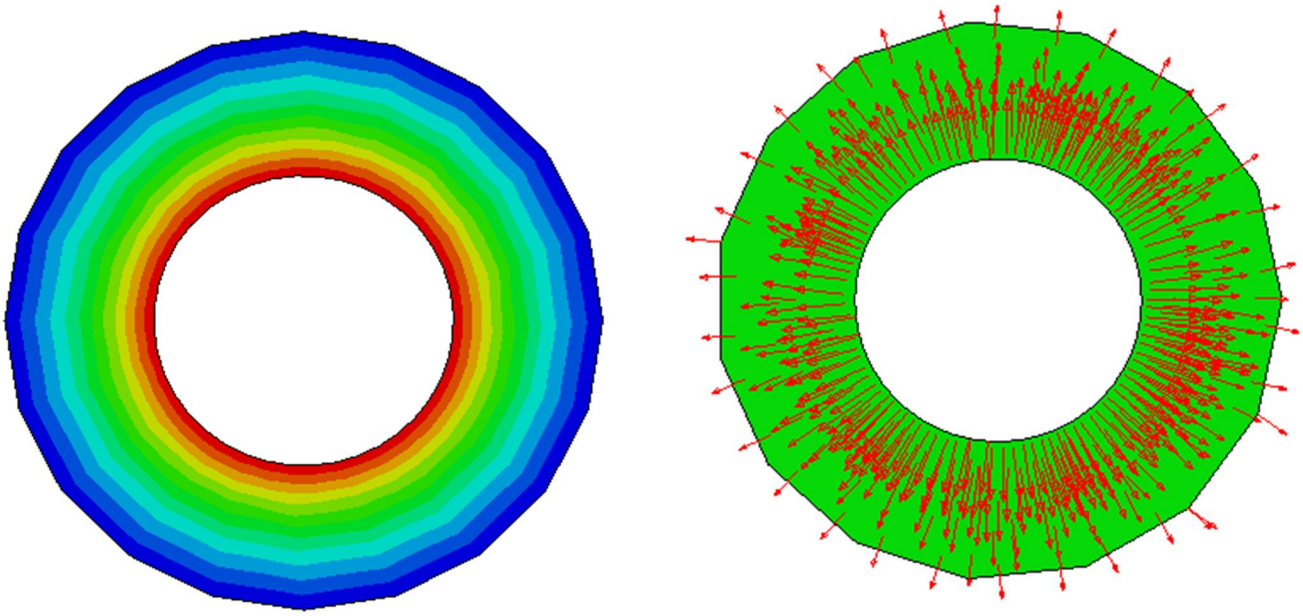

Figure 4.6: Showing how the membrane raptures as the temperature is increasing thereby releasing the heme out of the hemozoin. The layer close to the hemozoin i.e. the abdomen experiences the greater effect of the heat while, there is decrease of heat effect away from the hemozoin

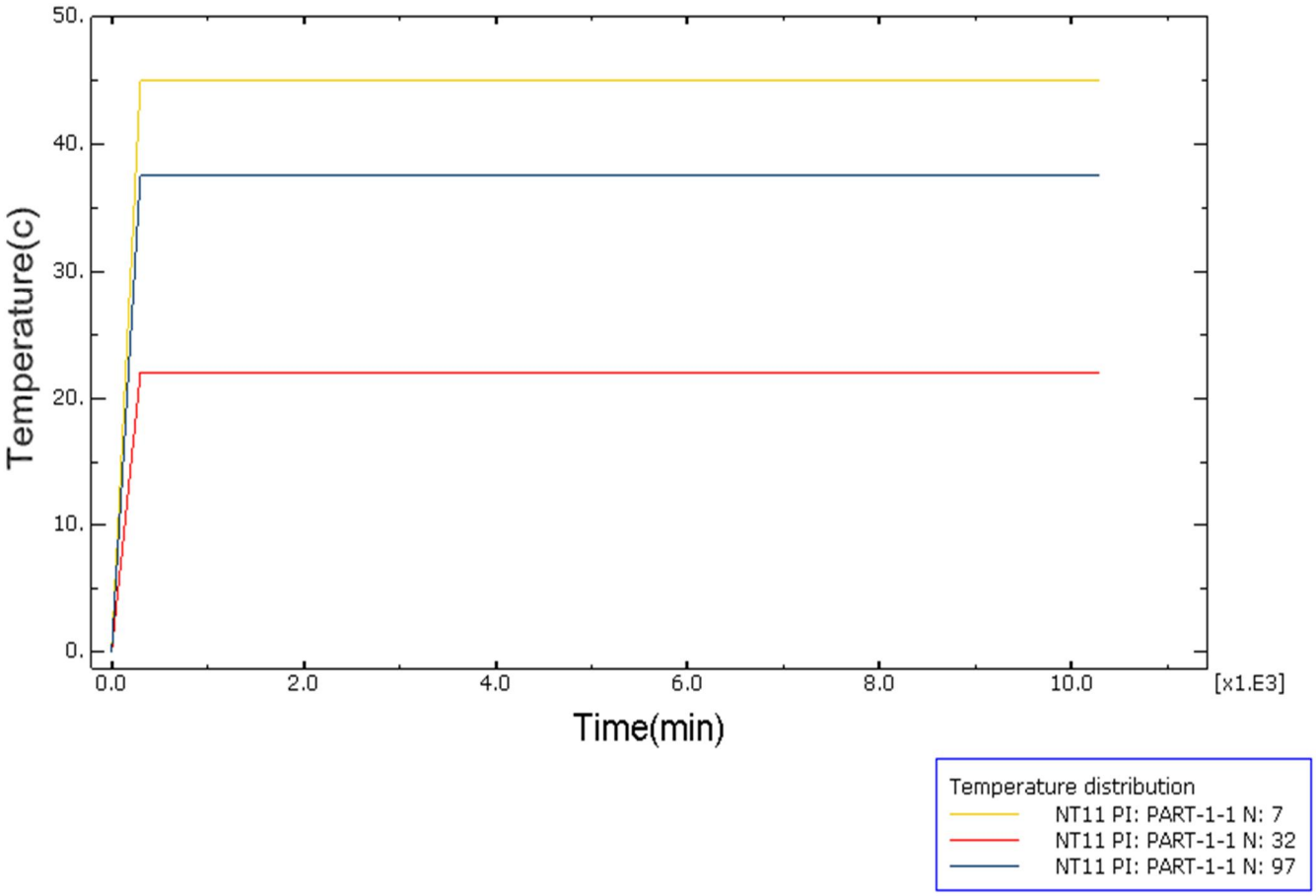

Figure 4.7: Showing the temperature distribution at the boundary of the hemozoin inside the abdomen of the parasite. Line N7 indicates the immediate effects of the heat since it the layer very close to the membrane followed by line 32 and then line 97 which is the body temperature of the mosquito

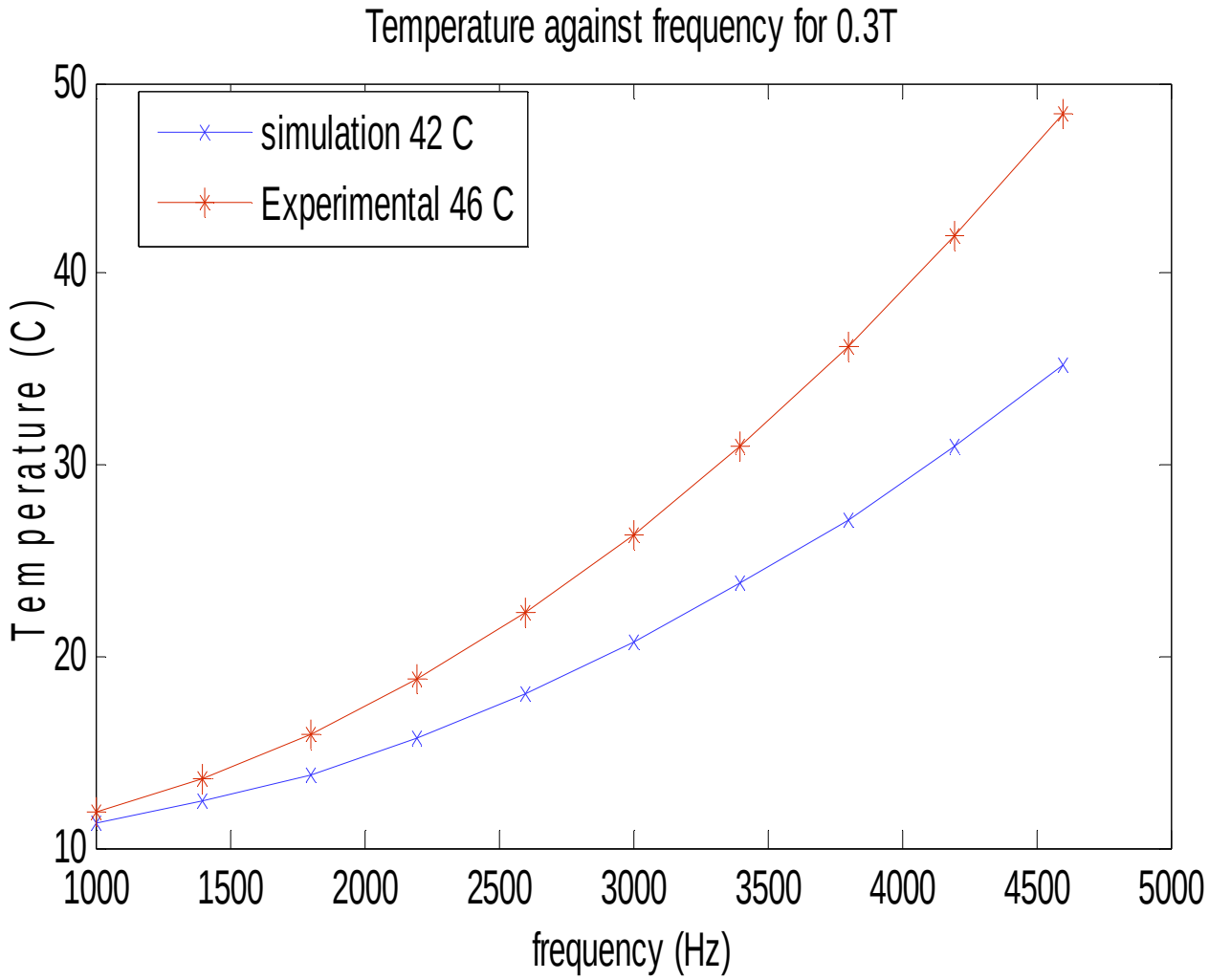

4.8: The temperature variation against frequency for 900 sec. This graph shows a trend of increasing temperature with increasing frequency of the field.

4.7 Effect of Temperature with varying magnetic field Induction

For a low magnetic induction of 0.04 T, there is a decrease in the frequency of 1.8 kHz and a temperature of 280.23K. During the winter season, where the temperature falls below 7centigrade, the parasite cannot survive. This is evidence in an experimental work carried out by Leena Bharadwa [73]. The figures below shows the numerical results

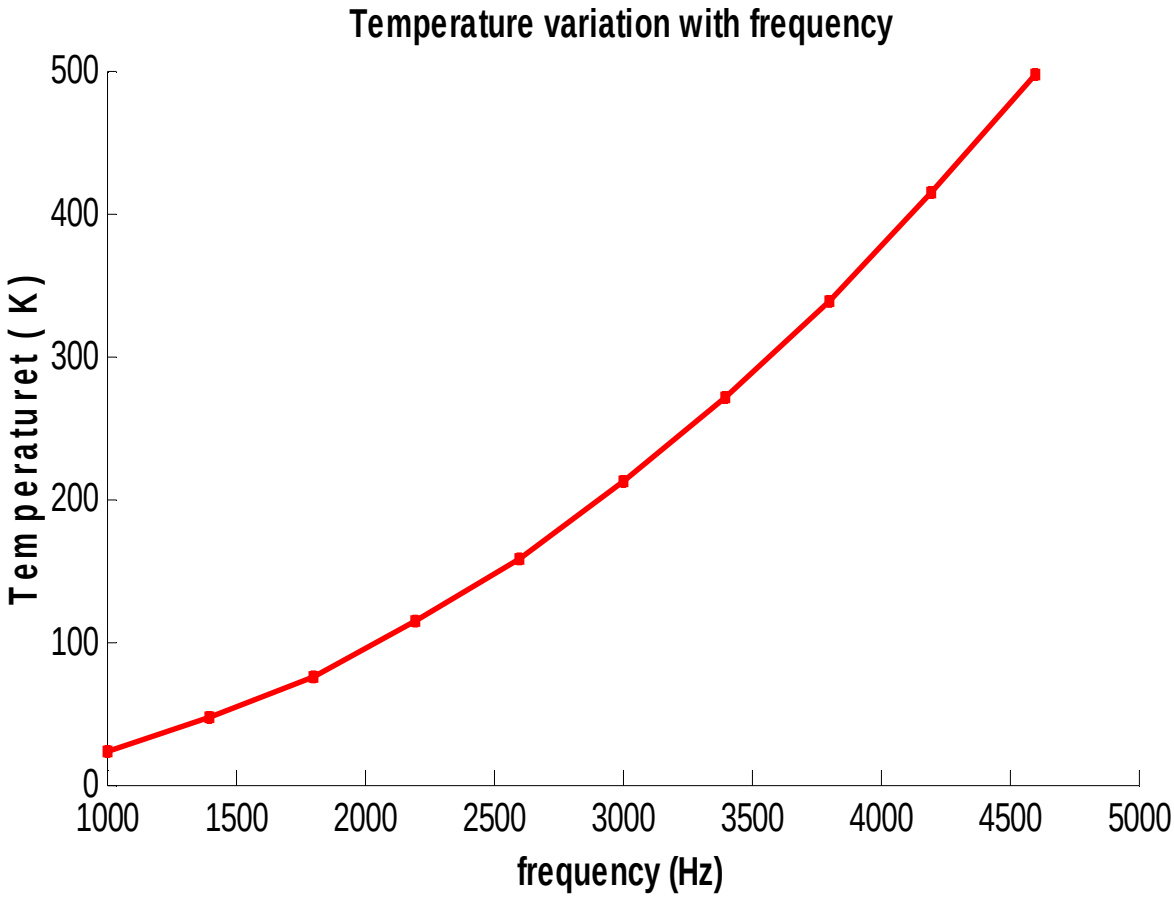

Figure 4.9 : Showing the temperature variation with respect to the frequency of the field

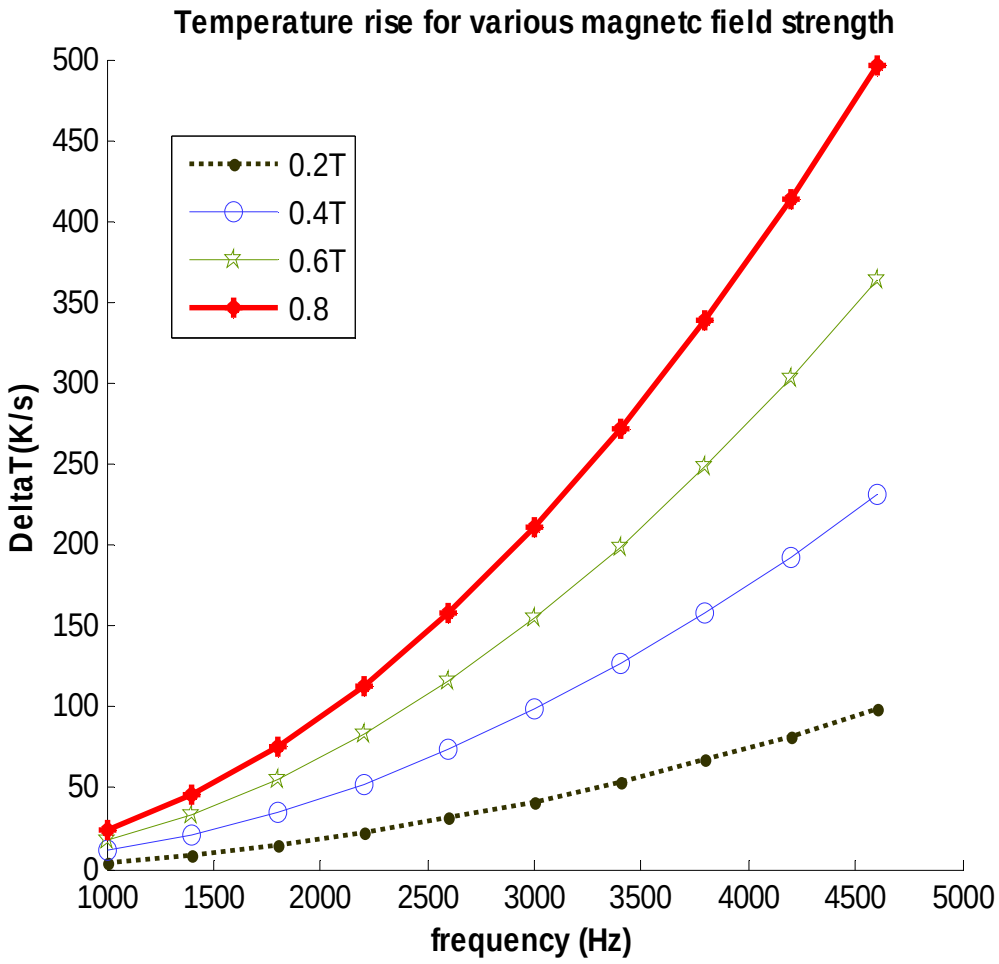

Figure 4.10 : Temperature vs frequency for different magnetic field intensity for 600s

4.8 Temperature distribution

The temperature distribution inside the heme and at the boundary of the hemozoin is of great importance. The numerical simulation was done using abacus in a 2D shell planar. An irregular shape was divided into a circular geometry, a process called discretization. Now, the next step was to give node numbers to each element and to specify the interpolation function for each. An element type was assigned for steady state in 900 s. The input parameters known as the material property are the thermal conductivity, the specific heat capacity and the density of the nanoparticle, in this case the goethite. The structural analysis uses the temperature as the loading so as to calculate the heat transfer from the heme to the boundary of the hemozoin. In our model, we consider two circles, where the inner circle contains the heme embedded inside the hemozoin and the outer circle, the internal abdomen of the mosquito. In order words, the heme is contained in the hemozoin. Here, we analyze the temperature distribution from the magnetic nanoparticle and across it boundaries. At a maximum temperature of 42^{o}C, for 900s steady state, the bonds in the particle begin to break off destroying their tertiary structure as a result of the thermal agitation in a form of collision thereby losing it ability to stay inside the chamber. This therefore enables the release of the nanoparticle out of the chamber of the hemozoin into the plasmodium falciparum making it inactive of malaria transmission.

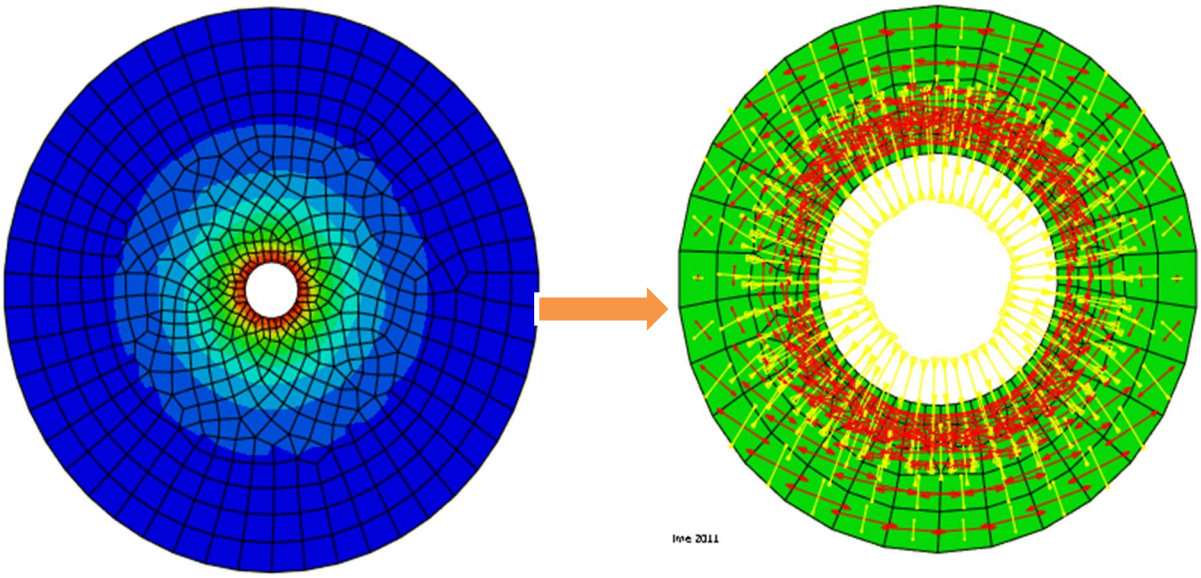

Figure 4.11: Application of the field causing vibration and collision resulting in generation of heat rupturing the heme out of the hemozin. We analyze the temperature distribution of irregular shape. This is the Contour profile showing the temperature distribution of an adiabatic boundary condition.

4.9 Discussion on the FEM

The finite element approximation was also used to investigate the reaction forces as well as the temperature distribution at each nodal point on the mesh. This analysis was useful in predicting the time it takes for the distribution of the temperature across the heme. It was observed that upon taking in the blood, the parasite body temperature rises from 22^{o}C to 33^{o}C, however, after feeding; the temperature reduces to room temperature within 300 sec.

4.10 Discussion on the Field

As the field is applied to the particle, they become magnetized in the direction of the field; however, demagnetization occurs in the absence of the field. Heat is dissipated as the particles undergo both the Brownian and the Ne'el relaxation process. The longer the time of exposure of the field to the plasmodium falciparum, the higher the frequency of the field and consequently the higher temperature, the particles are subjected to hence, the higher the rate of protein denaturing. In this case, the heme is easily release back into the system of the parasite from the hemozin and thus the parasite becomes weakens in it activities. Such a parasite can still bit but the rate of infecting with the malaria parasite is very low.

4.11 Collapse of the membrane of the Hemozoin

At low temperature, the spectral consist of sharp line inside the hemozoin, as the temperature is increasing, the line becomes broaden from the centroid of the spectrum and a doublet appears. At a temperature of 42^{o}C , the sextest and the doublet coexist and the spectrum collapses allowing the magnetic nanoparticle out of the chamber.

Chapter Five

5.1 Conclusion and Recommendation

From our numerical analysis, we determined the relationship between the frequency and the temperature of the field to be linearly dependent on each other. From the results and discussion, we concluded that, as the temperature increase, the frequency as well as the magnetic field induction also increases. At a stronger field induction of 0.3T, heme acquires enough to physically rotate in the hemozoin which was in the accordance with the experiment conducted by Solomon Abiola in Princeton. It was evident in the Abaqus simulation, we performed

At magnetic field of 1.5T, at 4.6 kHz, rapturing of membrane wall of the heomozoin and denaturing of the particle occurs. Therefore, we conclude that the plasmodium falciparum losses it activity at Tmax= 42 degC.
Termination of the malaria using electromagnetic field on human host could be recommended as future works. Pressure effects on the heme as they collide with each other could also be considered since we only investigated the temperature of the heme. A numerical and experimental analysis could also evaluate the stress component on the walls of the hemozoin.

References

[1] Kondrachine A.V Malaria in WHO Southeast Asia Region India J Malarial, 1992

[2] Olufunke A. Alaba Olumuyiwa B. Alaba , Malaria in Rural Nigeria: Implications for the Millennium Development Goals.

[3]WHO Global Malaria Programme WORLD MALARIA REPORT, 2010

[4] Global Malaria Action Plan

[5] Solomon O. Abiola, Helmholtz Coil Design for Non-Invasive Detection and Apoptosis of Breast Cancer and Malaria Parsites, via F e2O3, F e3O4 Nanoparticles and Hemin.

[6] Bupa's Health Information Team, Malaria- the disease, March 2010.

[7] Dr. Royal Raymond Rife Documentary Trailer, Magnetic Fields May Hold Key To Malaria Treatment – More Validity For Effectiveness Of Rife Machines On Microorganisms

[8] http://www.netdoctor.co.uk/travel/diseases/malaria_disease.htm

[9] APPMG, Tackle Malaria Today Increasing burden of poverty Give tomorrow a Chance

[10]Gabbad A.S.A. Amira Ibrahim Ahmed B.Sc, In Public and Environmental Health.1991 U.K. PhD thesis Universiy of Khartoum 2009

[11] Wernig F.and Xu Q 202, Mechanical stress -induced apoptosis in the cardiovascular system progress in Biological and Moluclar Biology,78(2), pp.105-137.

[12] Yoed Rabin, Cancer Treatment by Electromagnetic Activated Nanoheaters. Department of

[13]Robin D.Powell,Colonel Willam D. Tigertt ,Drug resistance of parasite causing Human Malaria

[14] http://en.wikipedia.org/wiki/ Hysteresis

[15]NDT Resoruce center

[16] Electronic Tutorial about Magnetic Hysteresis

[17] Lauren M. Blue1, Mary Kathryn Sewell1, Dong-Hyun Kim, Ph.D.1, Christopher S. Brazel, Ph.D. Fluid Dynamics and Heating of Magnetic Nanoparticles in Simulated Blood Vessels

[18] Q A Pankhurst, J Connolly, S K Jones and J Dobson "Applications of magnetic nanoparticles in biomedicine''

[19] Brown W.F. Jr 1963, Thermal Fluctuation of single -domain particle , Phys. Rev 130, 16787

[20]L. Rast and J. G. Harrison"Computational Modeling of Electromagnetically Induced Heatin of Magnetic Nanoparticle Materials for Hyperthermic CancerTreatment", Department of Physics, University of Alabama at Birmingham, Birmingham, Alabama 35294, USA

[21] N.Pamme, Magnetism and Microfluidics, Lab on chip 6(2006), 24-28

[22] Nils Z. Danckwardt, Matthias Franzreb, Andreas E. Guber, Volkersaile, Pump- Free transport of magnetic particle in microfluidic channels.

[23]C. Phatak, R. Pokharel, M. Beleggia, M. De Graef ,On the magnetostatics of chains of magnetic nanoparticles

[24] P. Tartaj, M.D Morales, S. Veintemilla- Verdaguer, T. Gonzales- Carreno, C.J. Serna, The preparation of Mahnetic nanoparticle for the appication in biomedicine, Journel of Phyics D-Applied Physics , 36(13)(2003) R182-R197

[25] Rosensweig Exxon, Heating Magnetic Fluid with Alternating Magnetic Field , Research and Engineering Co. (ret), 34 Gloucester Red, Summit, NJ07901, USA.

[26]RJD Tilley (2004). Understanding Solids. Wiley. p. 368. ISBN 0470852755.

[27]Griffiths, David J. (1999). *Introduction to Electrodynamics* (3rd ed.). Prentice Hall. pp. 222–225. ISBN0-13-805326-X. OCLC40251748.

[28]Richard Fitzpatrick Classical Electromagnetism: An intermediate level course

[29] Scott Hughes, Massachustts Institute of Technology, department of Physics, 8.022 Spring 2004. lecture 10; Magnetic force. Magnetic fields, ampere's law

[30] Landau , Lifshitx, The Classical theory of filed, Vol 2, 4th ed,1994, pp57.

[31] Henry C. Lai1 and Narendra P. Singh, Department of Bioengineering, University of Washington, Seattle, WA 98195-5061, USA.

[32] Olivia, Difference between oscillation and vibration

[33] Time Dependent Mechanical Behaviour.

[34]Robin D.Powell,Colonel Willam D. Tigertt ,Drug resistance of parasite causing Human Malaria.

[35] Wernig F.and Xu Q 202, Mechanical stress -induced apoptosis in the cardiovascular system

Washington, Seattle, WA 98195-5061, USA

[36]Prof. Dr. David J. Sullivan Jr Hemozoin: a BiocrystalSynthesized during theDegradation of Hemoglobin,The Malaria Research Institute, W. Harry Feinstone Department of Molecular Microbiology and Immunology, Bloomberg School of Public Health, Johns Hopkins

[37] A.-H. Lu, E. L. Salabas and F. Schüth, Angew. Chem., Int. Ed., 2007, 46,1222–1244 ^

[38]An-Hui Lu; E. L. Salabas, and Ferdi Schth (2007). *Angew. Chem. Int. Ed.* 46: 1222–1244.

[39]Wang X. et al. Application of Nanotechnology in Cancer Therapy and Imaging. CA Cancer J

[40]Joerg Lehmann and Brita Lehmann, Nanoparticle Thermotherapy: A New Approach in cancer Therapy

[41] Z.Li, M. Kawashita, N. Araki, M.Mistumori and M. Hiroka: Effect of particle size on Magnetite Nano-particle on Heat Generating Ability under Alternating Magnetic Field

[42] Henry C. Lai1 and Narendra P. Singh, Department of Bioengineering, University of Washington, Seattle, WA 98195-5061, USA

[43]Richard Fitzpatrick,Classical Electromagnetism: An intermediate level course

[44] Gerald W. Recktenwald, Finite-Difference Approximations to the Heat Equation

[45] Ziegler, J. Linck, R., and Wright, D.W(2001) Heme Aggregation inhibitors: antimalarial drugs targeting an essential biomineralization process, Curr Med Chem. 8,171-189

[46]Rudzinska, M.A.., Trager, W., and Bray, R. S(1965) Pinocytotic uptake and the digestion of haemoglobin in malaria parasites..,J. Protozoa 12,563.

[47] Hayward, R..,Saliba, K.J., and Kirk, K.(2006) The pH of the digestive vacuole of the plasmodium falciparum is not associated with chlorquine resistance , J CellSci119, 1016-1025.

[48] C. Wongsrichanalai, M. J. Barcus, S. Muth, A. Sutamihardja, and W. H. Wernsdorfer, "A review of malaria diagnostic tools: microscopy and rapid diagnostic test (RDT)," Am. J. Trop. Med. Hyg. **77**(6 Suppl), 119–127 (2007).

[49]Sullivan DJ (December 2002). "Theories on malarial pigment formation and quinoline action". *Int J Parasitol* **32** (13): 1645–53]

[50] Goldberg, D.E.(1998) Haemoglobin Degradation in plasmodium – Infected Red Blood Cells, Semin Cell Biol. 4,355

[51] Anh N. Hoang Hemzoin: A case of Heme Crystal Engineering

[52] Egan, T. J., Combrinck, J. M.,Egan, J.,Hearne, G. R.,Margues, H.M.,Ntenteni, S.,Sewell, B.T., Smith, P. J., Taylor, D.,Van Schalkwyk, D. A., and Walden, J .C (2002) Fate of heam iron in the malaria parasite plasmodium falciparum , Biochem J. 365, 343-347

[53] A. Dorn, S. R. Vippayunta, H. Matile, A, Blubendarf, J. L. Vennerstorm and R. G. Ridley, Biochem, Pharmacoal, 55 (1998)

[54] Chou and Fitch, 1998; Slater and Cerami 1992. Heme Polymerase Activity and the Stages specifically of Antimalarial Action of Chloroquine

[55] Ponka , P. (1999) Cell Biology of Heme, Am J Med Sci. 318, 241- 256

[56] Fitch , C .D ., and Kanjannanggulpan , P. (1987) The state of ferriportoporphyrin IX in malaria pigment , J Biol Chem 262, 15552 – 15555

[57] Chang, HH; Falick, A M;Carlton, PM; Sedat, J W;DeRisi; Marletta, MA. N-terminal processing of protein exported by malaria parasite. Mol Biocehm, Parasitol 2008,160,107 – 15

[58] Jacquin C. Niles , Joesph L. DeRisi and Michael A. Marletta , Inhibiting plasmodium falciparum growth and heme detoxification pathway using heme- binding DNA aptamers

[59] La'szlo' Smeller, Judit Fidy, The Enzyme Horseradish Peroxidase Is less compressible at higher pressure, Institute of Biophysics and radiation Biology, Semmelweis University, Budapest H-14444, Hungary

[60] [Kungui et al., 1997; Mozhaev et al., 1996

[61] Panick et al., 1999; Balmy et al., 1992

[61] Eva Natividad, Miguel Castro, and Arturo Mediano, Adiabatic magnetothermia makes possiblethe study of the temperature dependence of the heat dissipated by magnetic nanoparticles under alternating magnetic fields

[62] Clare K. Carney, S. Reese Harry, Sarah. L. Sewell, David W .Wright; Detoxification Biominerals

[63] Gigel Nedelcu, Magnetic nanoparticles impact on tumoral cells in the treatment by magnetic fluid hyperthermia

[64] Kannan M. Krishnan, Biomedical Nanomagnetics: A *Spin* Through Possibilities in Imaging,

Diagnostics, and Therapy

[65] Usami A, Tanaka M, Yoshikawa Y, Watanabe K, Ohtsuka H, Orino K. Heme-mediated binding of α-casein to ferritin: evidence for preferential α-casein binding to ferrous iron.

[66] Dunkov BC, Zhang D, Choumarov K, Winzerling JJ, Law JH. Isolation and characterization of mosquito ferritin and cloning of a cDNA that encodes one subunit.

[67] Kasyutich, O.; Ilari, A.; Fiorillo, A.; Tatchev, D.; Hoell, A.; Ceci, P. (2010). "Silver Ion Incorporation and Nanoparticle Formation inside the Cavity ofPyrococcus furiosusFerritin: Structural and Size-Distribution Analyses". *Journal of the American Chemical Society* **132** (10): 362

[68] Rachel Casiday and Regina Frey; Iron Use and Storage in the Body:Ferritin and Molecular Representations *Iron in Biology: Study of the Iron Content in Ferritin, The Iron-Storage Protein.*

[69] S P Gubin, Yu A Koksharov, G B Khomvtov, G Yu Yurkov, Magnetic nanoparticle ;preparation, structure and properties

[70] L. Rast and J. G. Harrison, Computational Modeling of Electromagnetically Induced Heating of Magnetic Nanoparticle Materials for Hyperthermic Cancer Treatment

[71] M.P.Pileni, Nanocrystal formation mesoscopic structures

[72] M. Mohapatra, and S. Anand, Synthesis and application of nanostructured iron oxides/hydroxides

[73] Yu. L. Rackher and V. I. Stepanov, Magnetic relaxation in a suspension of Antiferromagnetic Nanoparticles

[74] Leena Bharadwaj , Kritika Trigunayat & Madan Mohan Trigunayat Thermal characterization of

APPENDIX

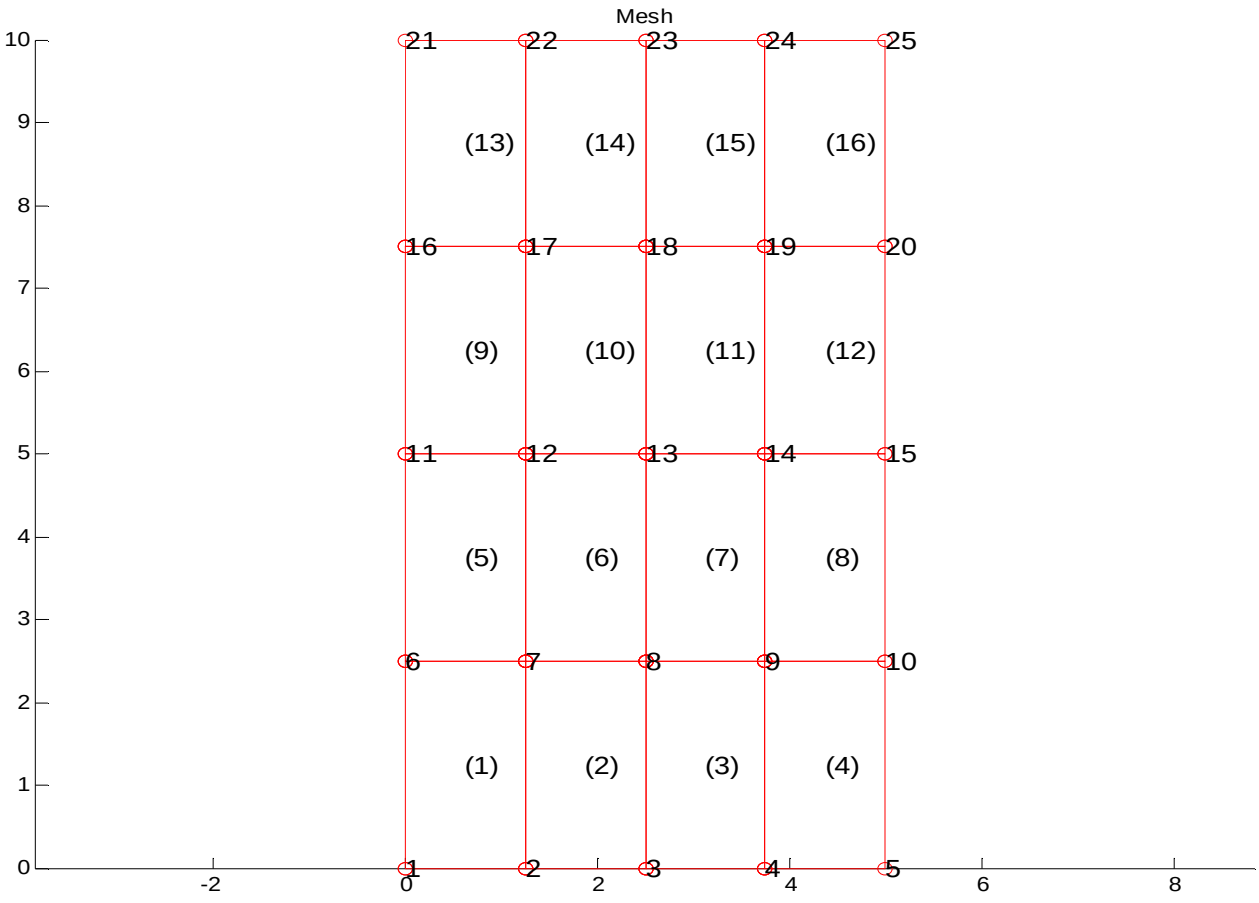

Figure 1: A finite element discretization in 2D of a rectangular mesh

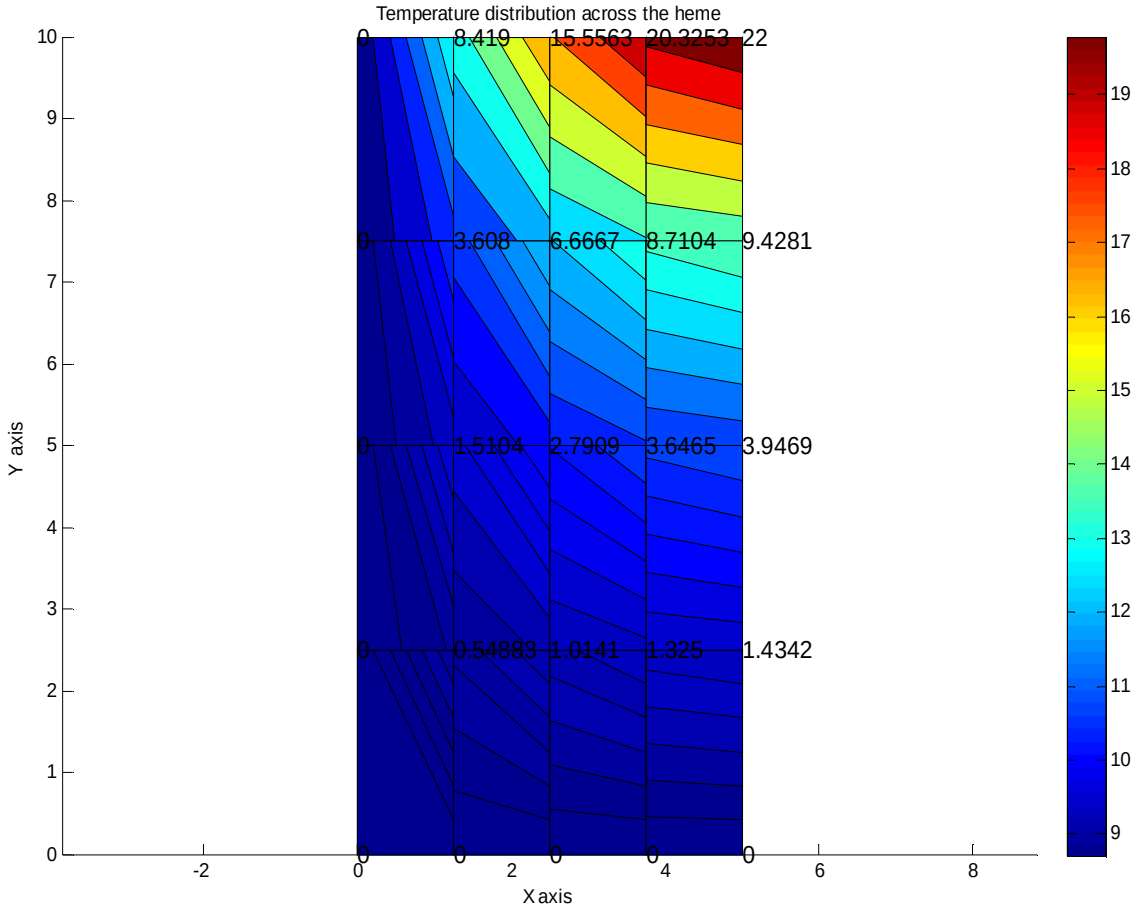

Figure 2 : The temperature distribution at each nodal point in the mesh

The Malta Code for the Temperature distribution

```
t = 1800;                    %exposure time
C = 738;                   %specific heat of matrix at fixed volume fraction
Kb = 1.38*10^-23;                %Boltzman constant
T = 315;                      %Body temperature of the tissue
%eta = 0.001;                  %viscosity in Pa.s ie 1000cs
Md = 446*10^3;                        % Domain magnetization
Vm = 2.6808e-025;
mu = 4*pi*10^-7;                          %permeability of free space
```

```
teff = 4.1303e-011;                                  %effective relaxation time

Phi = 0.05;                                         %volume fraction of
nanoparticles

Chi = 0.2569;

Bo=[0.2:0.2:0.8]                                                    %initial
susceptibility

%H = [1000:1400:13600];                              %amplitude of field

f = [1000:400:4950];

 DeltaT = zeros(10,10);                             %frequency

for i = 1:10                                      %loop for various field strenghts

    B = Bo(i);

    %H_1=H(i);

     Ho = B/mu

    H = Ho/sqrt(2)

                                                    %field strength

    xi = mu*Md*H*Vm/(Kb*T);                          %Langevin parameter

    Chi0 = Chi*(3/xi)*(coth(xi)-(1/xi))             %Static susceptibility

                                                     %DeltaT for different
frequencies

    for j = 1:10                                     %loop for various
frequencies

        w = f(j);

        P = mu*pi*Chi0*Ho^2*w*2*pi*w*teff/(1+(2*pi*w*teff)^2);     %power
dissipation

        DeltaT(i,j) = P*(t/C);                                    %Temperature
rise

    end

    plot(f(1,[1:10]),DeltaT(i,[1:10]),'-k^'); %hold all

    %;tittle('Temperature rise againts frequency')

    %ylable('Temperature(k)')

   % xlable('frequency(Hz)')
```

```
    xlabel('frequency (Hz)')
     ylabel('Heat(^\circ K)')
     %ylabel('DeltaT(K/s)') ;%hold all
     %format short e
      meshgrid(Bo,f,DeltaT);
      %DeltaT= peaks(f,Bo);
      %mesh(Bo,f,DeltaT)
     %[X,Y] =meshgrid(-10:.125:10);
     %z = peaks (X,Y);
     %mesh(X,Y,Z)
     % [f,Bo] = meshgrid(-1:.125:9);
%Z = peaks(X,Y);
%mesh(X,Y,Z)
end
```